Rice husk-templated hierarchical porous TiO_2/SiO_2 for enhanced bacterial removal

Dalong Yang [a,1], Bin Du [b,1], Yaxian Yan [b], Huiqin Li [c], Di Zhang [a] and Tongxiang Fan [a,*]

[a] State Key Laboratory of Metal Matrix Composites, Shanghai Jiaotong University, Shanghai, 200240, P.R. China

[b] School of Agriculture and Biology Department, Shanghai Jiaotong University, Shanghai, 200240, P.R. China

[c] Instrumental Analysis Center, Shanghai Jiaotong University, Shanghai, 200240, P.R. China

* Corresponding author. Tel.: +86-21-54747779; Fax: +86-21-34202749

Email address: txfan@sjtu.edu.cn

[1] Authors who contributed equally.

Supporting Information

Experimental Section

Characterization of the microstructure of the samples

The micro-mesoporous images of cross sections of the samples together with three-dimensional images of the samples were observed using atomic force microscopy (AFM, Mulitimode Nano Scope III a).

The macroporous images of cross sections of the samples were collected on conductive glass slides. They were sputtered with gold and observed using field mission scanning electron microscopy (FESEM, NOVA Nano SEM 230).

The BH-TiO_2/SiO_2 was suspended in ethanol by ultrasonic treatment and then dropped onto copper grids. The samples were examined using a transmission electron microscope (TEM, JEOL 2100F) at an applied voltage of 200 kV.

The surface areas and micro-mesopore-size distributions were evaluated by nitrogen-adsorption measurements, operated at 77 K on a Micromeritics ASAP 2020 adsorption analyzer. All of the samples originating from the rice husk were degassed at 300^oC and 10^{-6} Torr for 6 h prior to the measurements. The pore-sizes and distribution curves were derived from the adsorption isotherm by employing the Barrett-Joyner-Halenda (BJH) method, and the surface areas were calculated through the Brunauer–Emmett–Teller (BET) equation.

The porosity and macropore-size distributions were evaluated by a mercury porosimeter (Auto Pore IV 9510).

Characterization of the chemical component of the samples

The crystal phases of all of the samples were examined by X-ray diffraction (XRD) on a Bruker-AXS X-ray diffractometer system with Cu Kα radiation at 40 kV and 100 mA. The spectra were recorded in the 2θ range from 10^o to 90^o with a scanning step of 0.02^o/s. The average crystalline sizes were calculated by the Williamson-Hall method, expressed as follows: $\beta_i(\cos\theta_i)/\lambda = K/D+4\varepsilon(\sin\theta_i)/\lambda$, where β_i was the integral breadth (inradius 2θ) of the ith Bragg reflection peak positioned at $2\theta_i$; K was aconstant with the value of 0.89; λ = 0.154 nm was the wavelength of the X-rays; D was the average size of the crystallites; and ε was the microstrain, whose distribution was isotropic. D and ε were calculated through a least-squares fit.

Characterization of the physical properties of the samples

The particle sizes and zeta potentials of the samples were evaluated by photon correlation spectroscopy (Malvern Mastersizer 2000 and Malvern Zetasizer Nano S90). The temperature of characterization was 25^oC. The samples were dispersed uniformly in pure water by ultrasonic before characterization, and the concentrations of the samples were 0.01 g/L. The equilibrium time was 120 sec for each characterization, the run times of each characterization were 15, and the interval was 30 sec between interfacing characterizations. Each characterization

was repeated 3 times to avoid accident errors. Moreover, the zeta potential characterizations of the samples were tested in 5 different pH values as follows: 3, 5, 7, 9 and 11. The pH value was measured by a pH meter (PHS-3C) and monitored by HCl and NaOH.

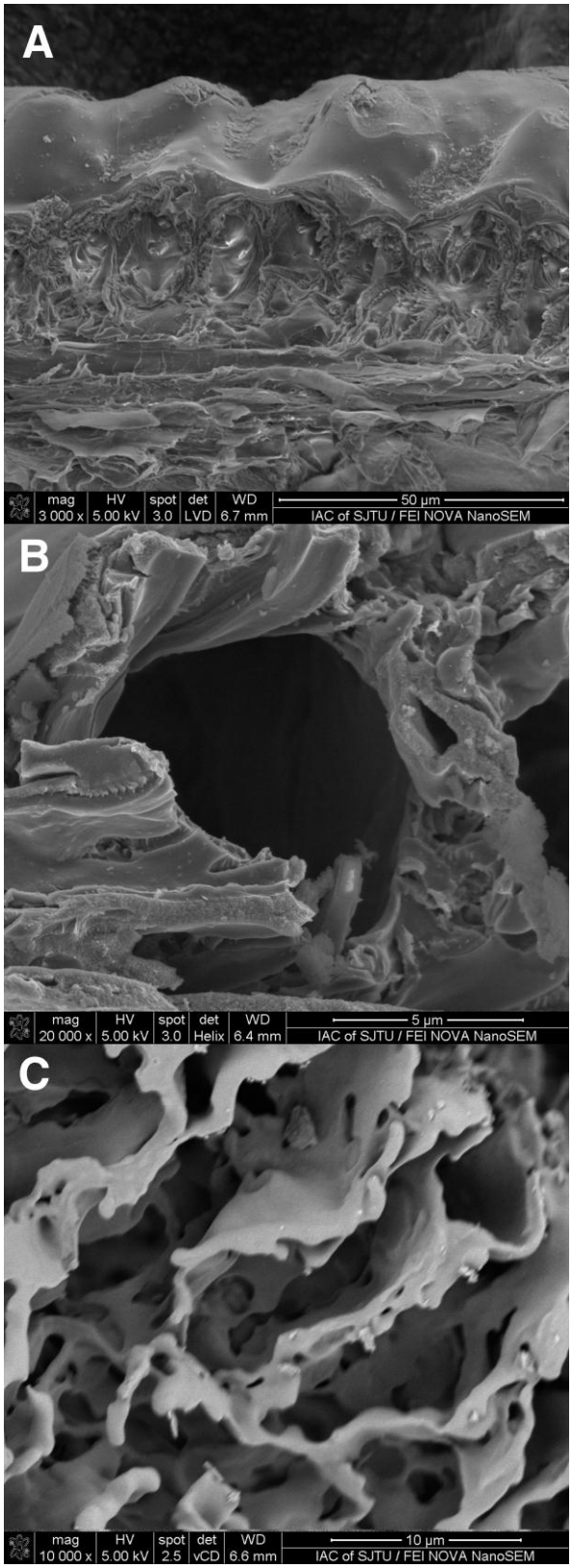

Figure S1. FESEM images of the cross-section of different samples. (A) Original rice husk; (B) BH-TiO_2/SiO_2; (C) Powdered activated carbon originating from rice husk.

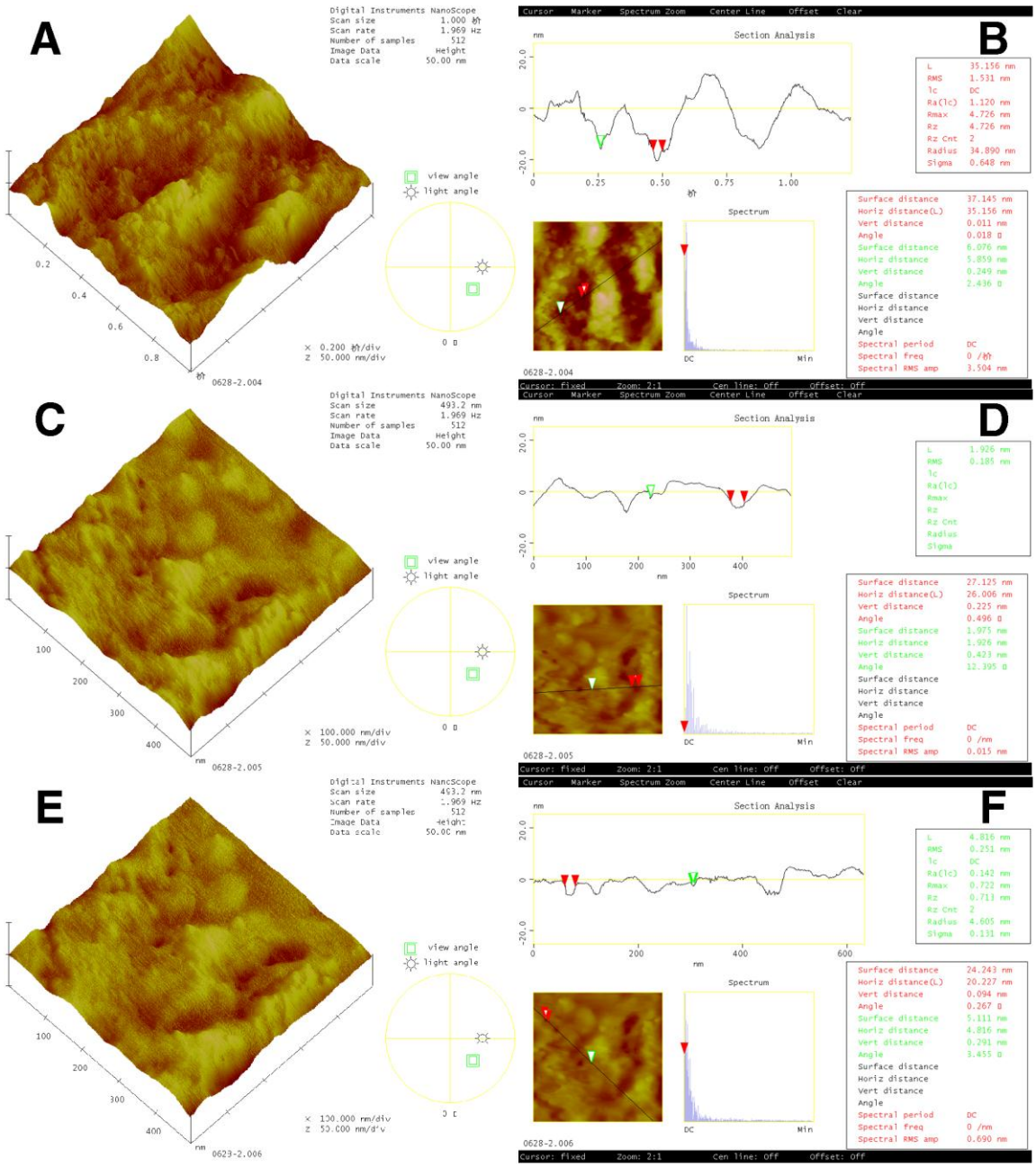

Figure S2. AFM 3D images of the cross-section of different samples. (A) Original rice husk; (C) BH-TiO_2/SiO_2; (E) Powdered activated carbon originating from the rice husk. The typical micro-mesoporous structure characterization of AFM images of the cross-section of different samples (the typical micro-mesopore could be found between 2 green and red triangles). (B) Original rice husk; (D) BH-TiO_2/SiO_2; (F) Powdered activated carbon originating from the rice husk. The bright parts correspond to higher features.

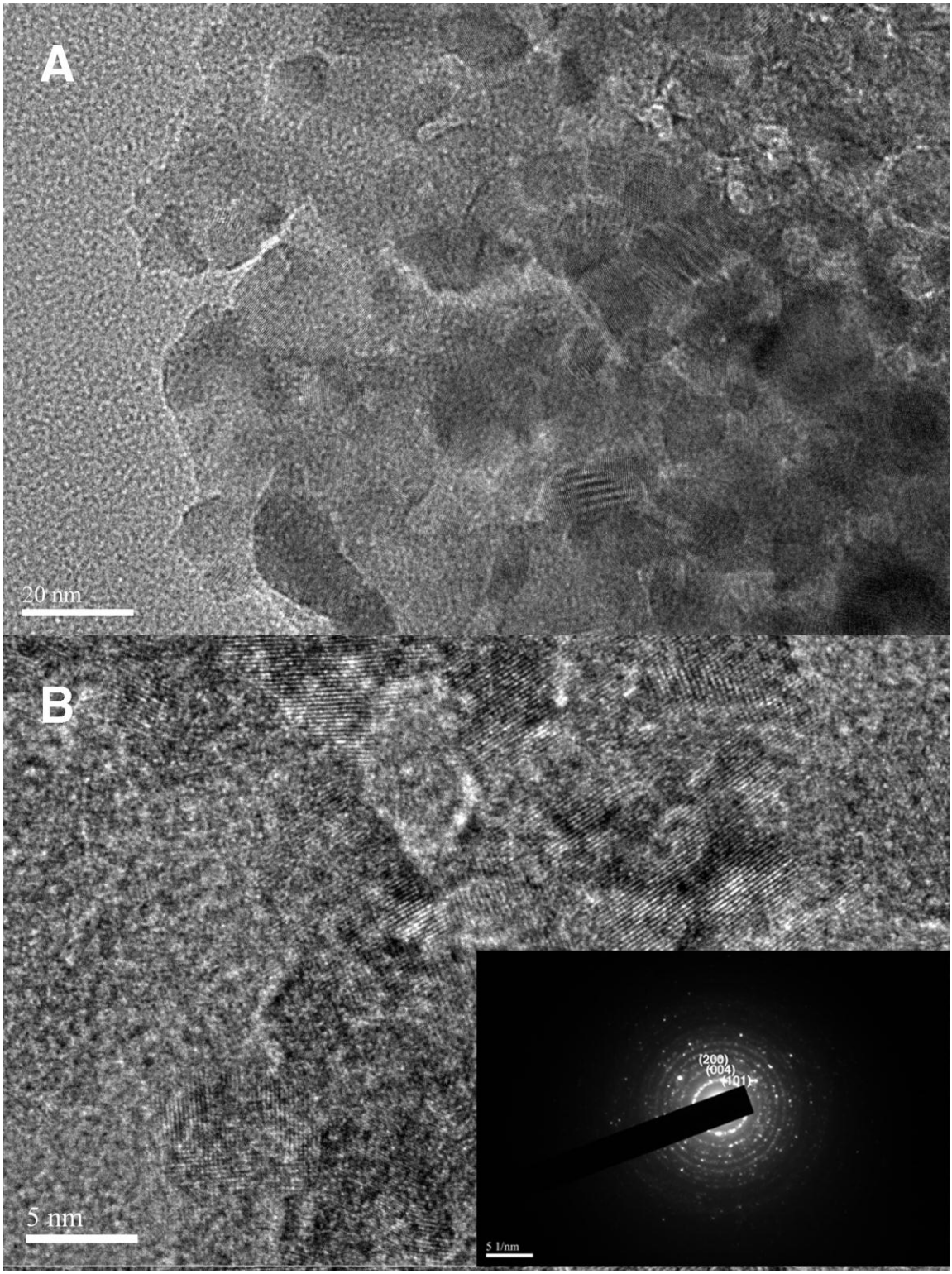

Figure S3. (A) TEM image of BH-TiO_2/SiO_2; (B) HRTEM image of BH-TiO_2/SiO_2, the inset shows the selected area electron diffraction (SAED) pattern.

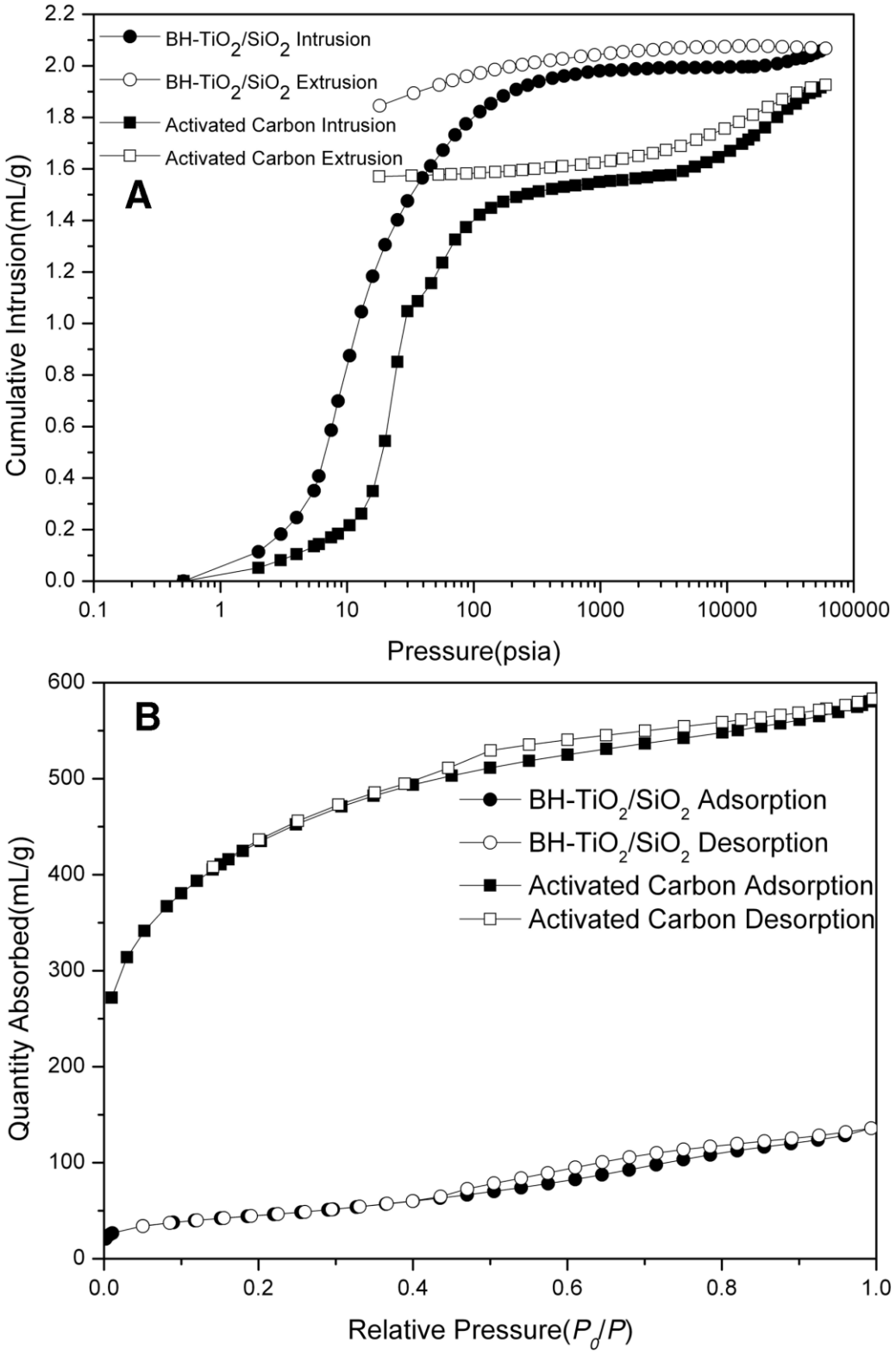

Figure S4. (A) The intrusion-extrusion isotherm of the samples originating from the rice husk measured by a mercury porosimeter. (B) The adsorption-desorption isotherm of the samples originating from the rice husk measured by nitrogen-adsorption measurements.

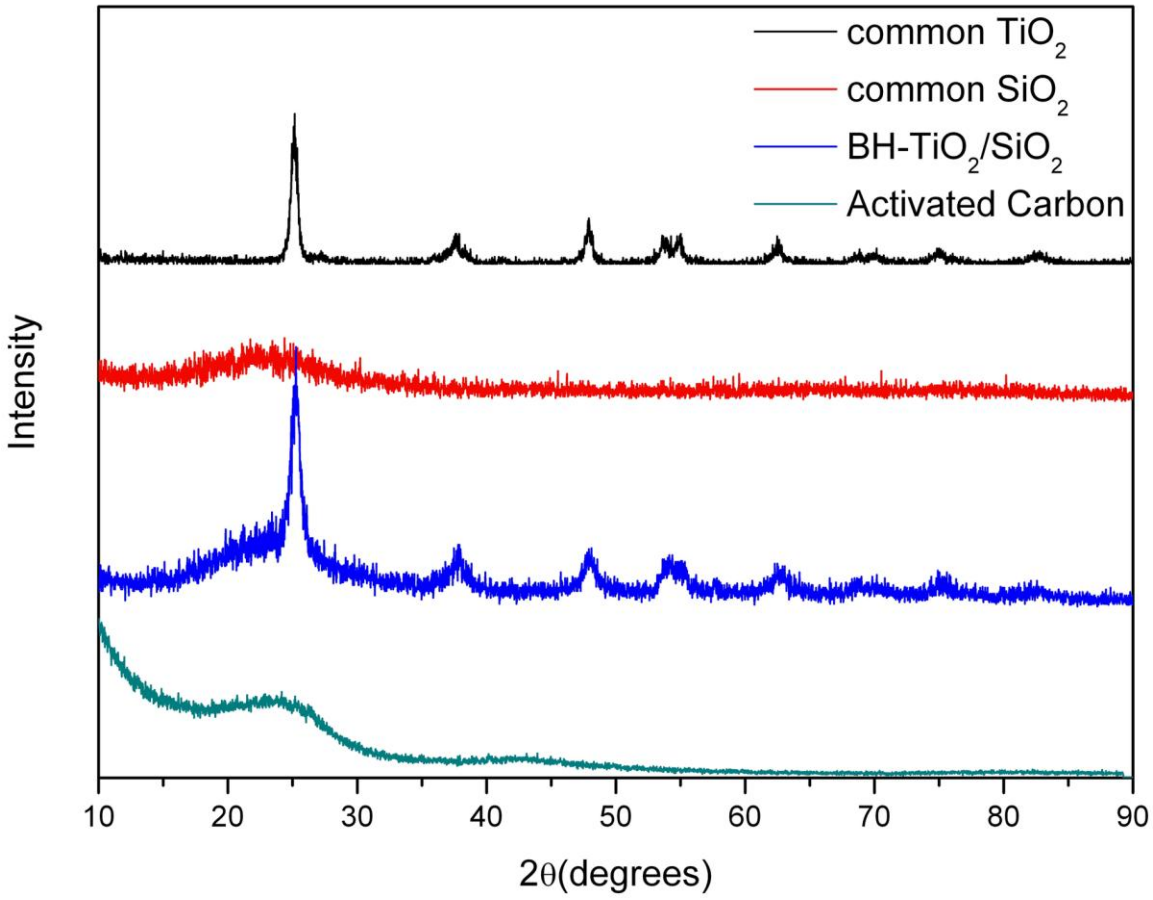

Figure S5. X-ray diffraction patterns of different samples.

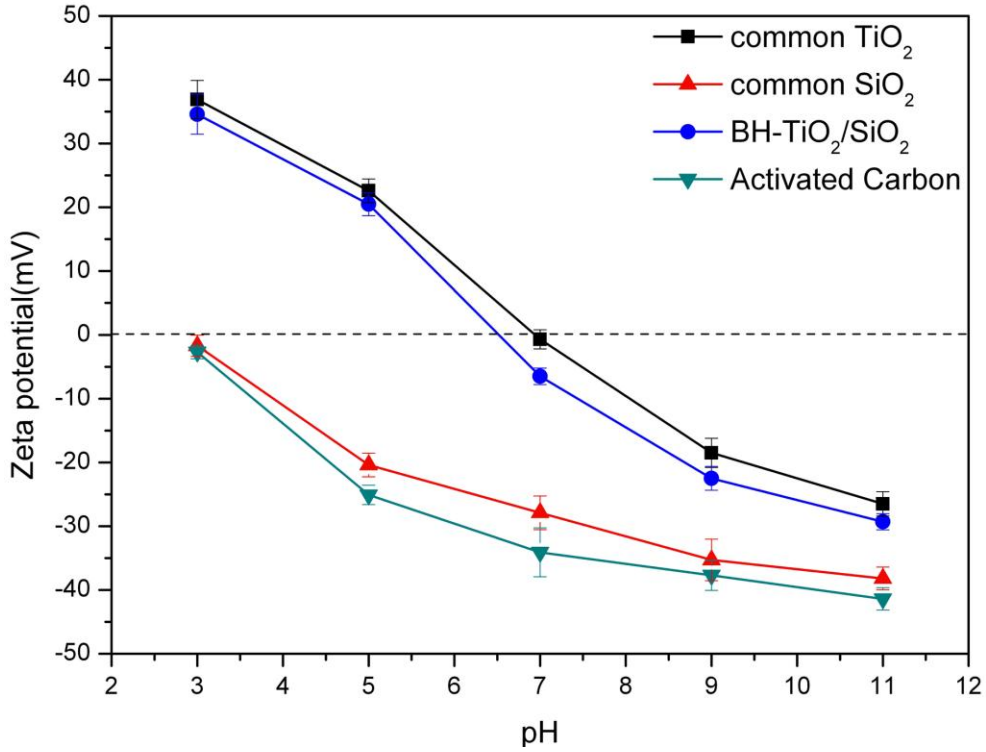

Figure S6. Zeta potentials of different ground samples under the different pH values.

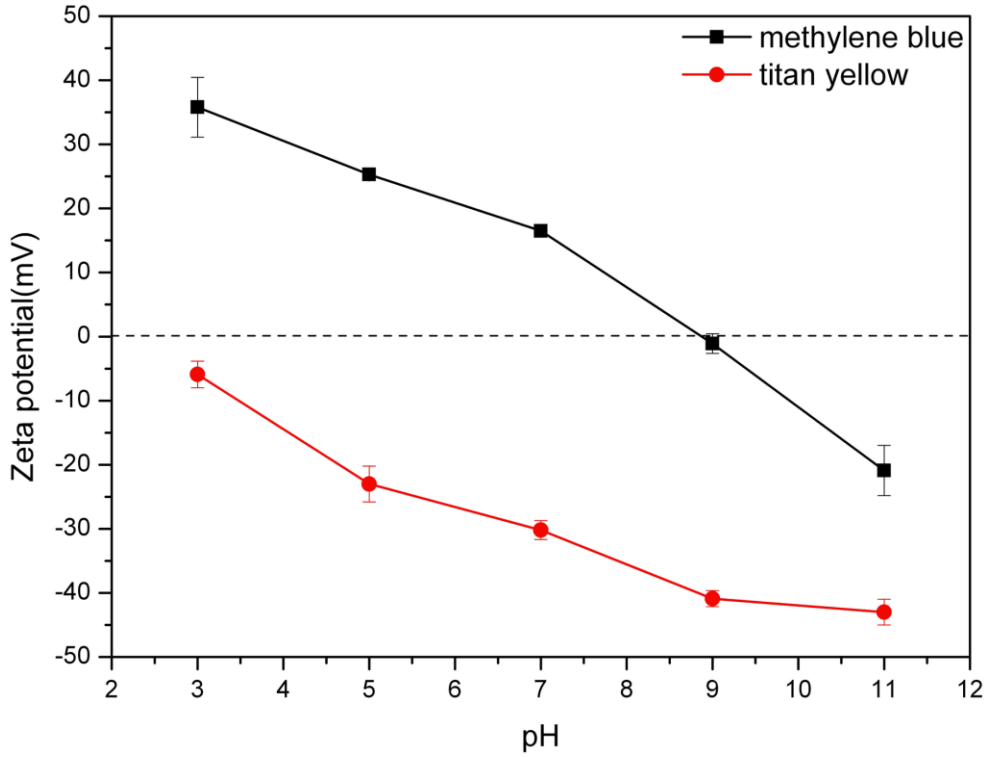

Figure S7. Zeta potentials of different dye solutions under the different pH values.

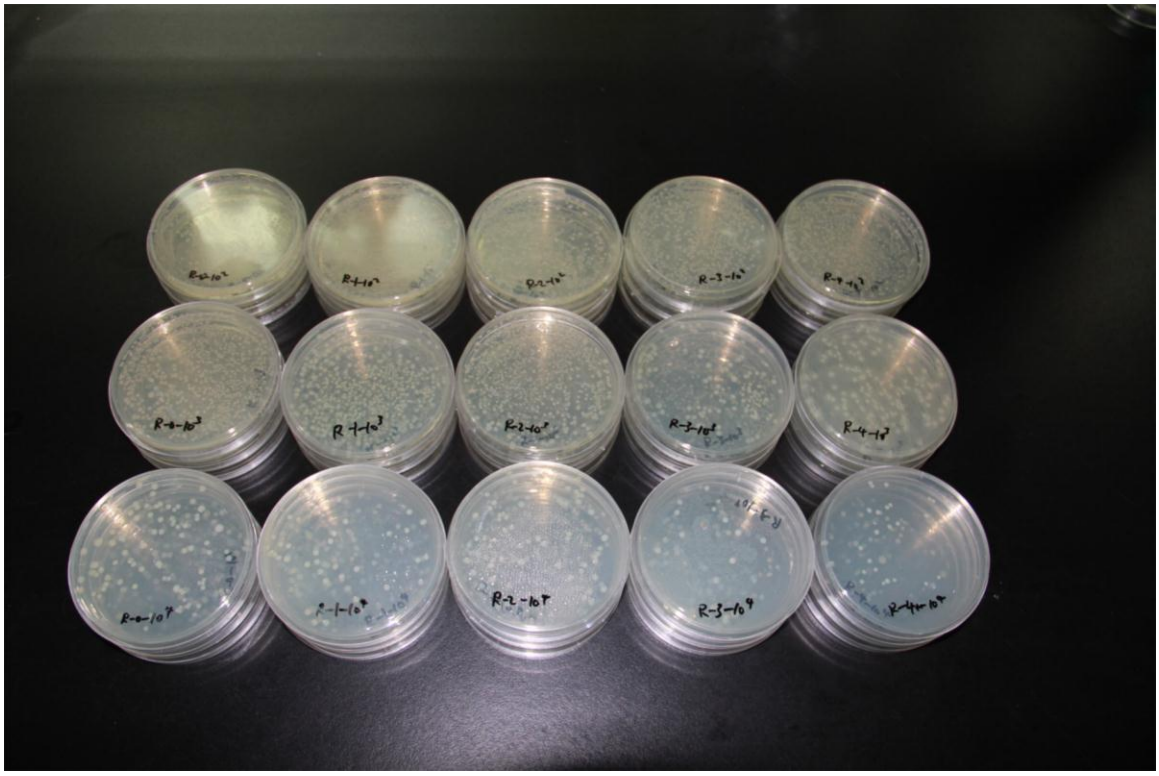

***Figure S8*.** Magnified images of *Escherichia coli* filtrate on LB agar plates. The filtrate has been diluted to 3 different times as 10^2, 10^3, and 10^4. Type R means *E. coli* physical removal experiment: Type 0 is the filtrate obtained without absorbents; Type 1 is the filtrate obtained under the adsorption effect of common TiO_2; Type 2 is the filtrate obtained under the adsorption effect of common SiO_2; Type 3 is the filtrate obtained under the adsorption effect of BH-TiO_2/SiO_2; Type 4 is the filtrate obtained under the adsorption effect of activated carbon originating from the rice husk.

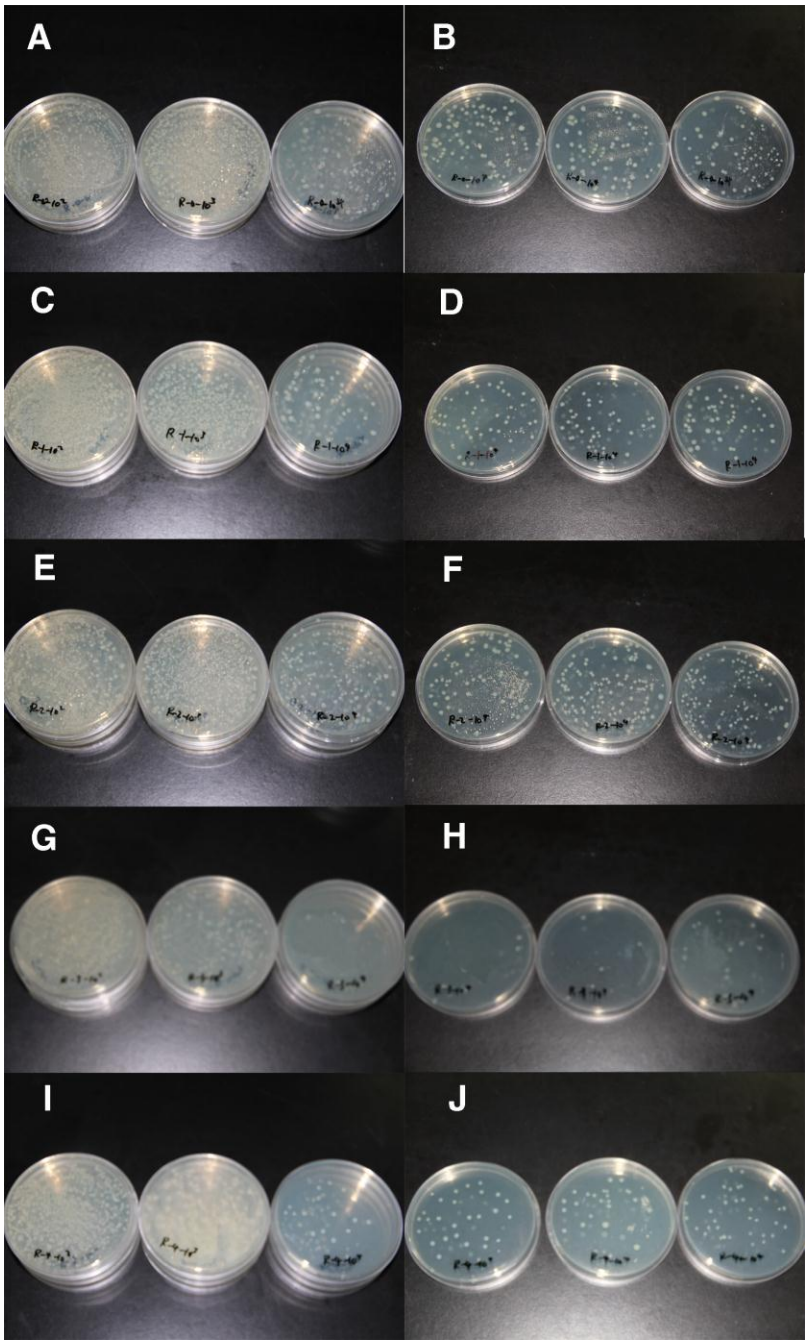

***Figure S9*.** Magnified images of *Escherichia coli* filtrate on LB agar plates. The filtrate has been diluted to 3 different times as 10^2, 10^3, and 10^4. Type R means *E. coli* physical removal experiment. (A) Type 0 is the filtrate obtained without absorbents; (C) Type 1 is the filtrate obtained under the adsorption effect of common TiO_2; (E) Type 2 is the filtrate obtained under the adsorption effect of common SiO_2; (G) Type 3 is the filtrate obtained under the adsorption effect of BH-TiO_2/SiO_2; (I) Type 4 is the filtrate obtained under the adsorption effect of activated carbon originating from the rice husk. (B), (D), (F), (H) and (J) The suitable plates for *E. coli* colony count are those diluted to 10^4.

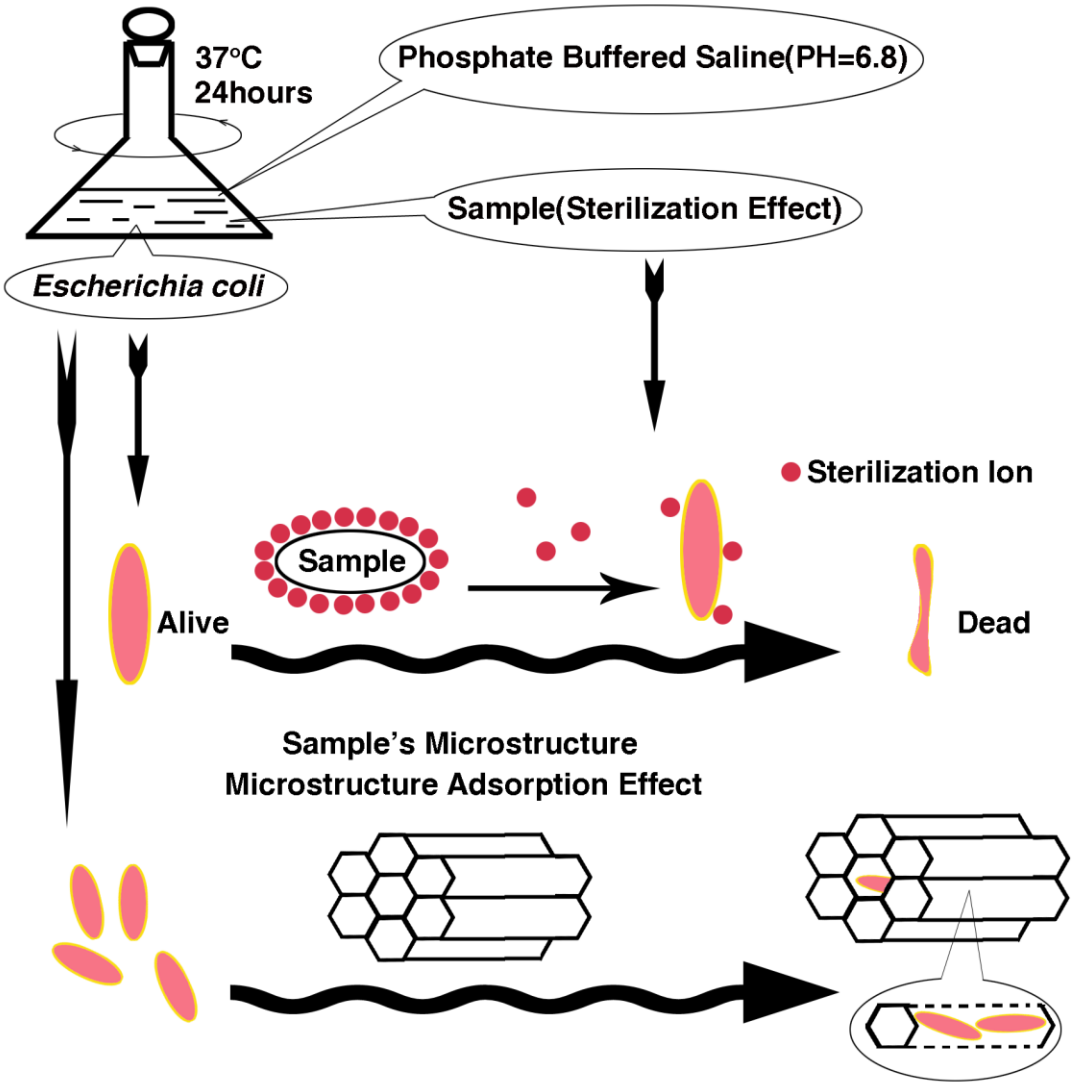

***Figure S10*.** The *Escherichia coli* bacteriostatic equipment and the potential mechanism for different samples' bacteriostatic properties.

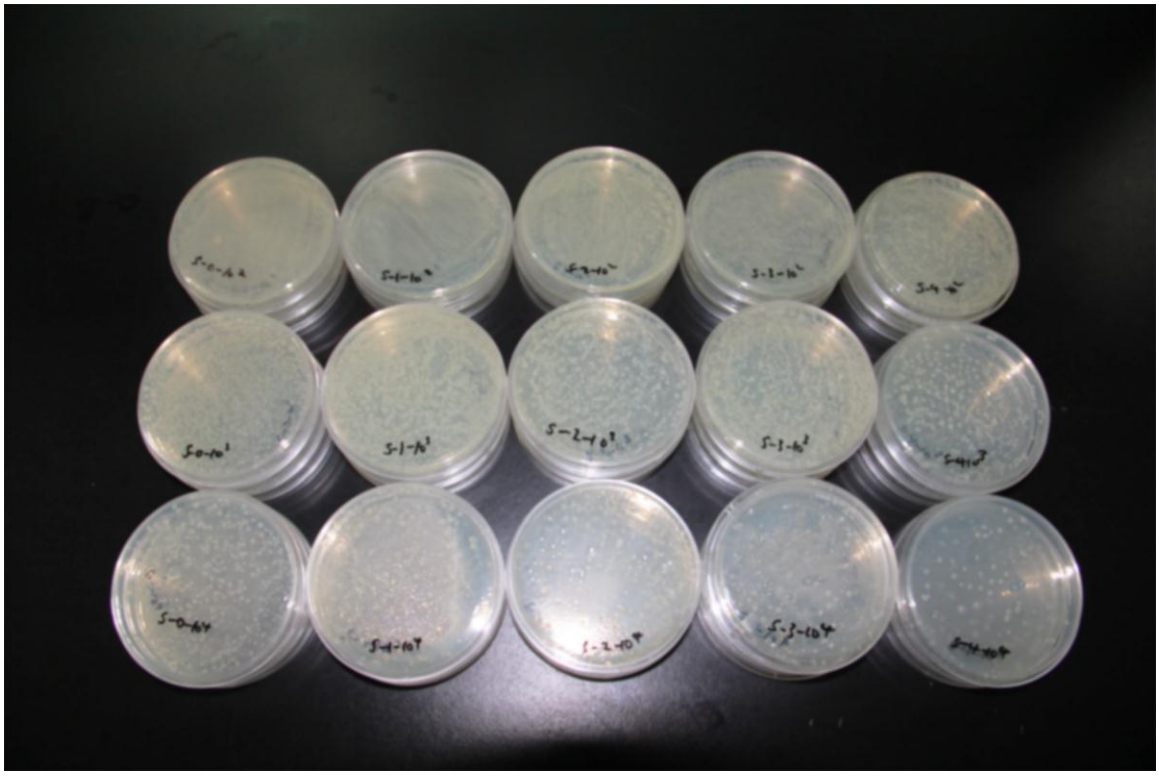

***Figure S11*.** Magnified images of *Escherichia coli* solution on LB agar plates. The solution has been diluted to 3 different times as 10^2, 10^3, and 10^4. Type S means *E. coli* sterilization (bacteriostatic) experiment. Type 0 is the solution that is not under the bacteriostatic effect of samples; Ttype 1 is the solution that is under the bacteriostatic effect of common TiO_2; Type 2 is the solution that is under the bacteriostatic effect of common SiO_2; Type 3 is the solution that is under the bacteriostatic effect of BH-TiO_2/SiO_2; and Type 4 is the solution that is under the bacteriostatic effect of activated carbon originating from the rice husk.

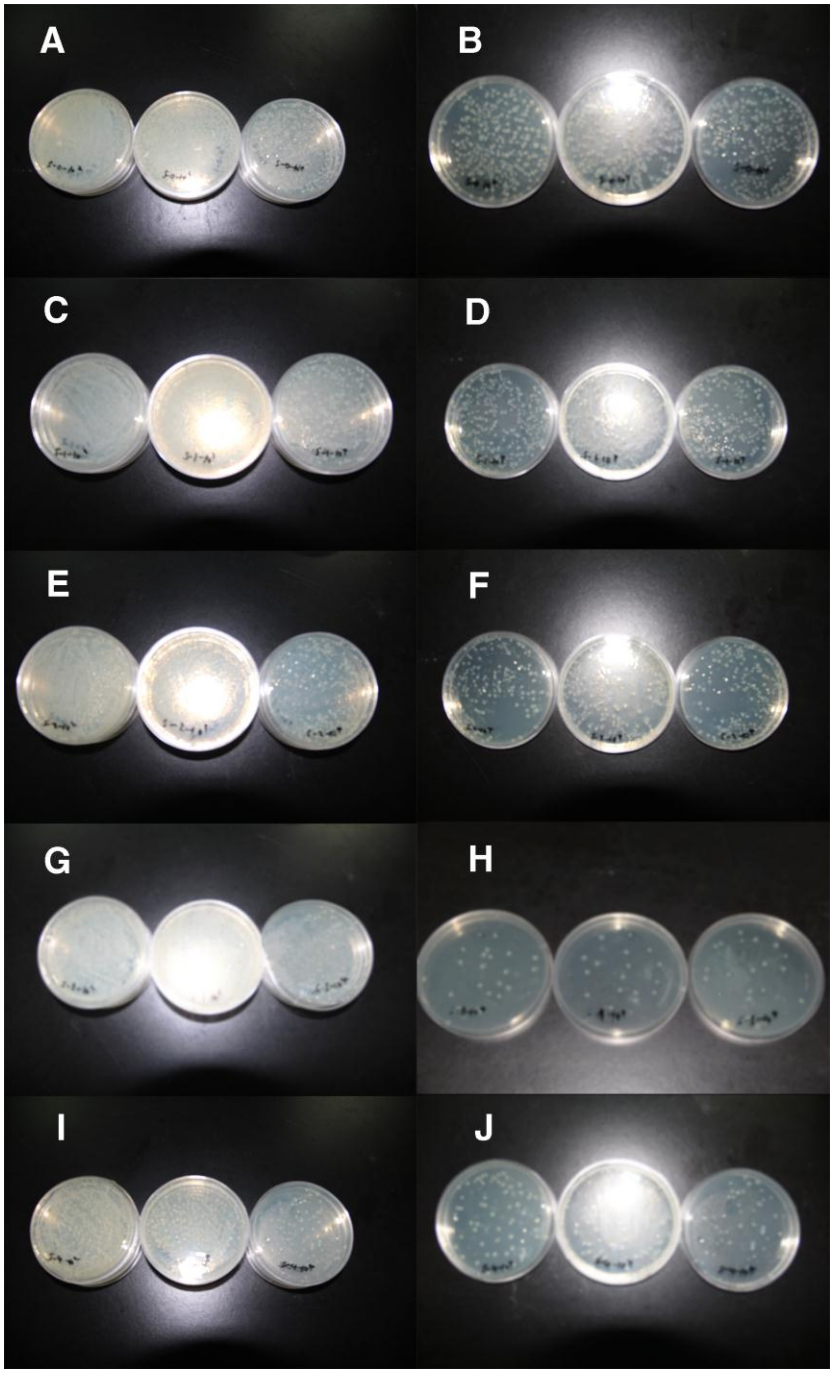

***Figure S12*.** Magnified images of *Escherichia coli* solution on LB agar plates. The solution has been diluted to 3 different times as 10^2, 10^3, and 10^4. Type S means *E. coli* sterilization (bacteriostatic) experiment. (A) Type 0 is the solution that is not under the bacteriostatic effect of samples; (C) Type 1 is the solution that is under the bacteriostatic effect of common TiO_2; (E) Type 2 is the solution that is under the bacteriostatic effect of common SiO_2; (G) Type 3 is the solution that is under the bacteriostatic effect of BH-TiO_2/SiO_2; (I) Type 4 is the solution that is under the bacteriostatic effect of activated carbon originating from the rice husk. (B), (D), (F), (H) and (J) The suitable plates for *E. coli* colony count are those diluted to 10^4.

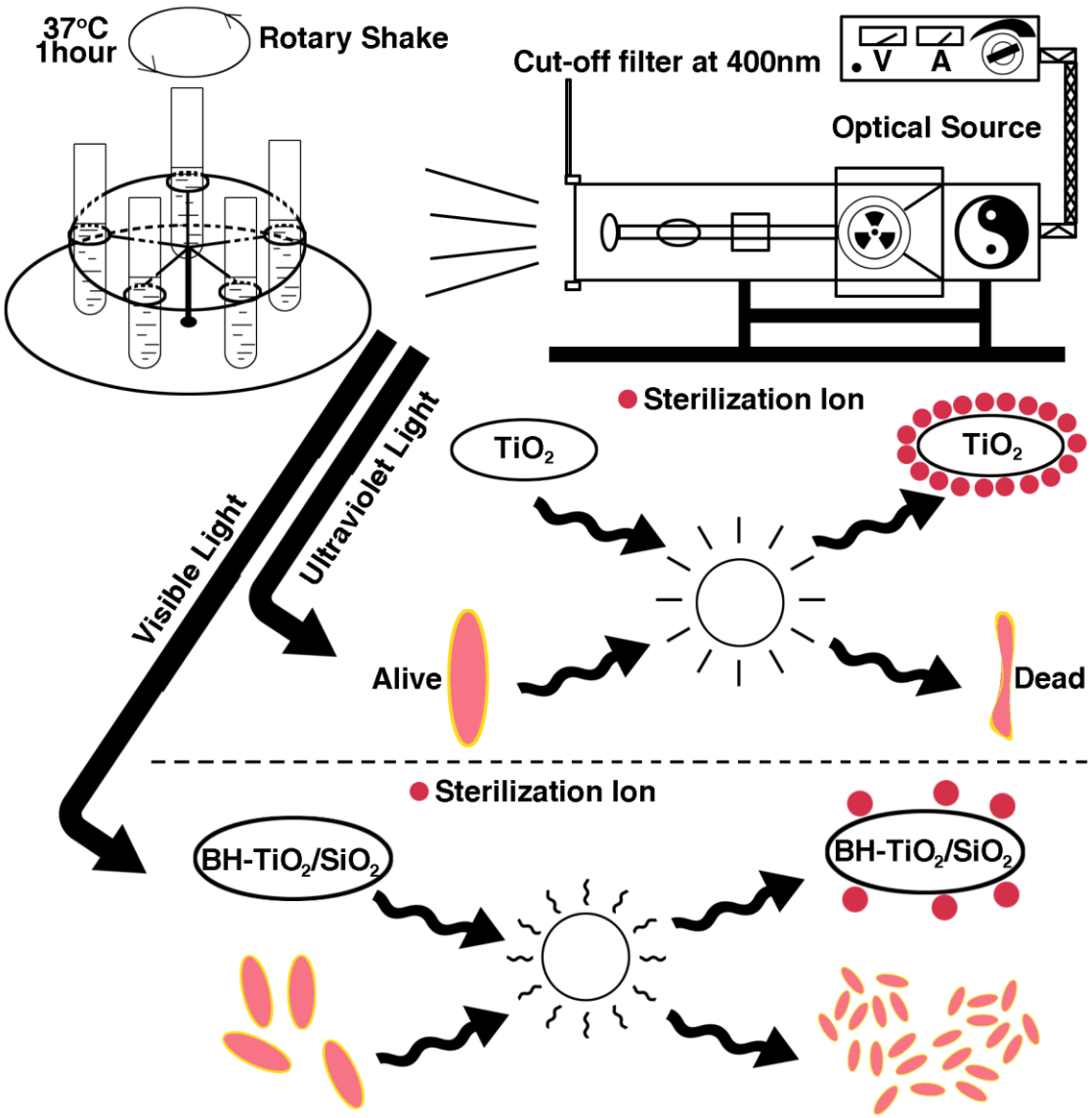

Figure S13. The equipment of *Escherichia coli* chemical removal properties of samples under light source and the potential mechanism for different samples' sterilization properties with *Escherichia coli* under UV or visible light irradiation.

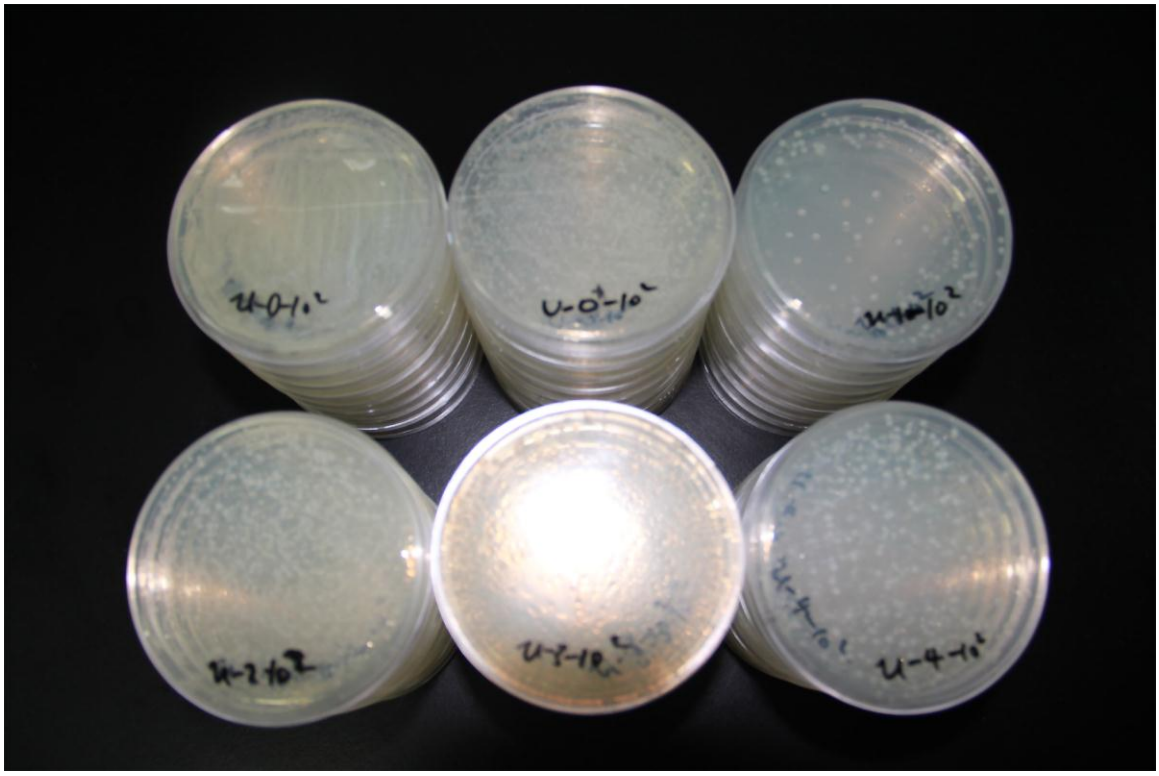

***Figure S14*.** Magnified images of *Escherichia coli* solution on LB agar plates. The solution has been diluted to 3 different times as 10^2, 10^3, and 10^4. Type U means *E. coli* sterilization experiment by different samples' photocatalytic properties under the UV irradiation. Type 0 is the solution without samples that is not under the UV irradiation; Type 0^+ is the solution without samples that is under the UV irradiation; Type 1 is the solution with common TiO_2 that is under the UV irradiation; Type 2 is the solution with common SiO_2 that is under the UV irradiation; Type 3 is the solution with BH-TiO_2/SiO_2 that is under the UV irradiation; and Type 4 is the solution with activated carbon originating from the rice husk that is under the UV irradiation.

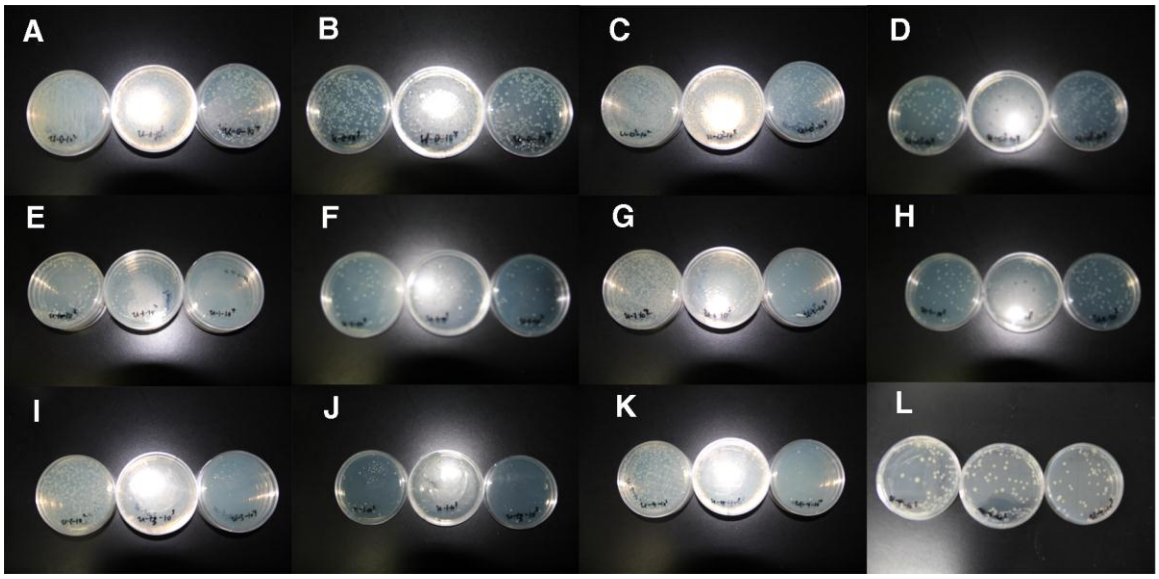

***Figure S15*.** Magnified images of *Escherichia coli* solution on LB agar plates. The solution has been diluted to 3 different times as 10^2, 10^3, and 10^4. Type U means *E. coli* sterilization experiment by different samples' photocatalytic properties under the UV irradiation. (A) Type 0 is the solution without samples before the UV irradiation; (C) Type 0^+ is the solution without samples that is under the UV irradiation; (E) Type 1 is the solution with common TiO_2 that is under the UV irradiation; (G) Type 2 is the solution with common SiO_2 that is under the UV irradiation; (I) Type 3 is the solution with BH-TiO_2/SiO_2 that is under the UV irradiation; (K) Type 4 is the solution with activated carbon originating from the rice husk that is under the UV irradiation. (B) and (D) The suitable plates for *E. coli* colony count are those diluted to 10^4. (F), (H), (J) and (L) The suitable plates for *E. coli* colony count are those diluted to 10^3.

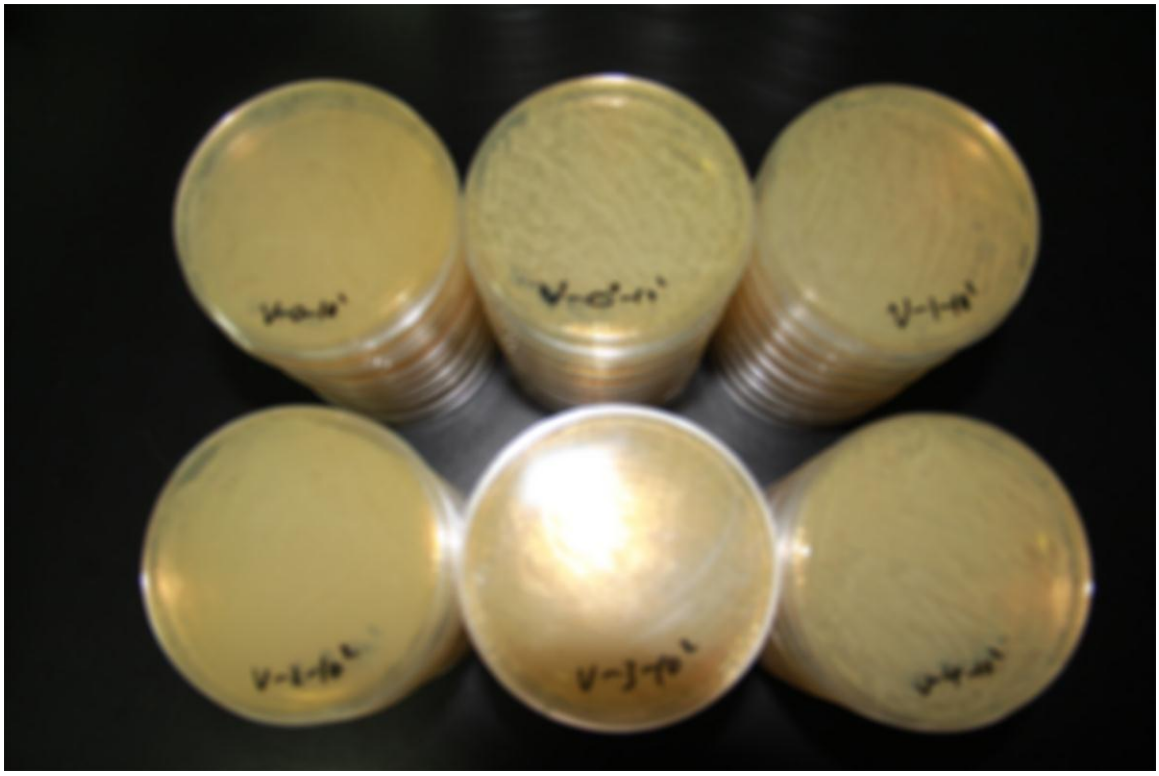

***Figure S16*.** Magnified images of *Escherichia coli* solution on LB agar plates. The solution has been diluted to 3 different times as 10^2, 10^3, and 10^4. Type V means *E. coli* sterilization experiment by different samples' photocatalytic properties under visible light irradiation. Type 0 is the solution without samples before the visible light irradiation; Type 0^+ is the solution without samples that is under visible light irradiation; Type 1 is the solution with common TiO_2 that is under visible light irradiation; Type 2 is the solution with common SiO_2 that is under visible light irradiation; Type 3 is the solution with BH-TiO_2/SiO_2 that is under visible light irradiation; and Type 4 is the solution with activated carbon originating from the rice husk that is under visible light irradiation.

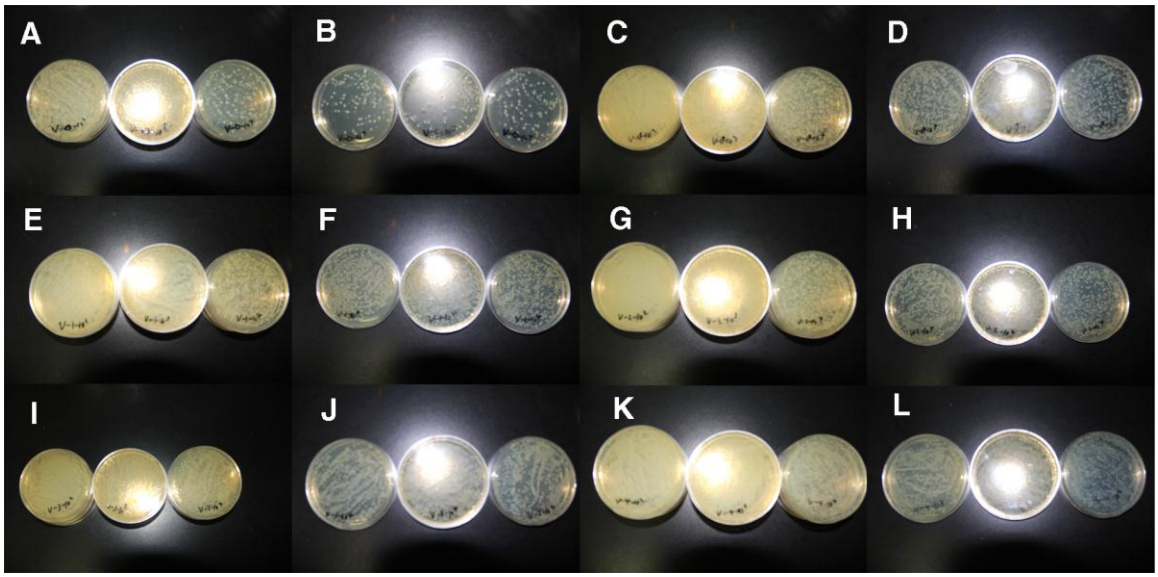

***Figure S17*.** Magnified images of *Escherichia coli* solution on LB agar plates. The solution has been diluted to 3 different times as 10^2, 10^3, and 10^4. Type V means *E. coli* sterilization experiment by different samples' photocatalytic properties under visible light irradiation. (A) Type 0 is the solution without samples before the visible light irradiation; (C) Type 0^+ is the solution without samples that is under visible light irradiation; (E) Type 1 is the solution with common TiO_2 that is under visible light irradiation; (G) Type 2 is the solution with common SiO_2 that is under visible light irradiation; (I) Type 3 is the solution with BH-TiO_2/SiO_2 that is under visible light irradiation; (K) Type 4 is the solution with activated carbon originating from the rice husk that is under visible light irradiation. (B), (D), (F), (H), (J) and (L) The suitable plates for *E. coli* colony count are those diluted to 10^4.

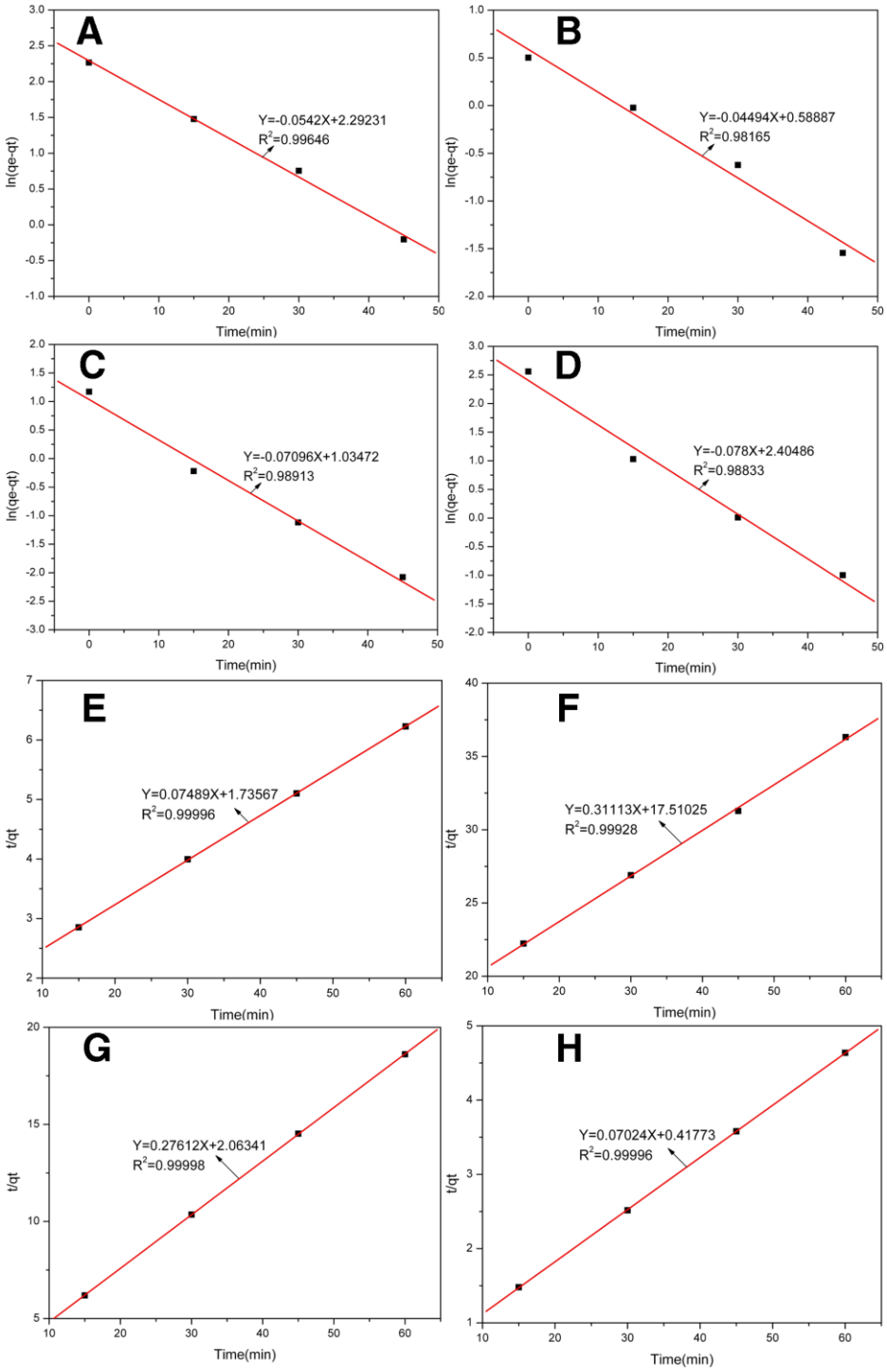

***Figure S18*.** Plots of pseudo-first-order and pseudo-second-order rates for different kinds of adsorbents and the adsorption of 25 mgL^{-1} titan yellow dye solution. The former 4 figures were fit to the pseudo-first-order model, and the latter 4 figures were fit to the pseudo-second-order model. (A) Common TiO_2; (B) Common SiO_2; (C) BH-TiO_2/SiO_2; (D) Activated carbon originating from the rice husk; (E) Common TiO_2; (F) Common SiO_2; (G) BH-TiO_2/SiO_2; (H) Activated carbon originating from the rice husk.

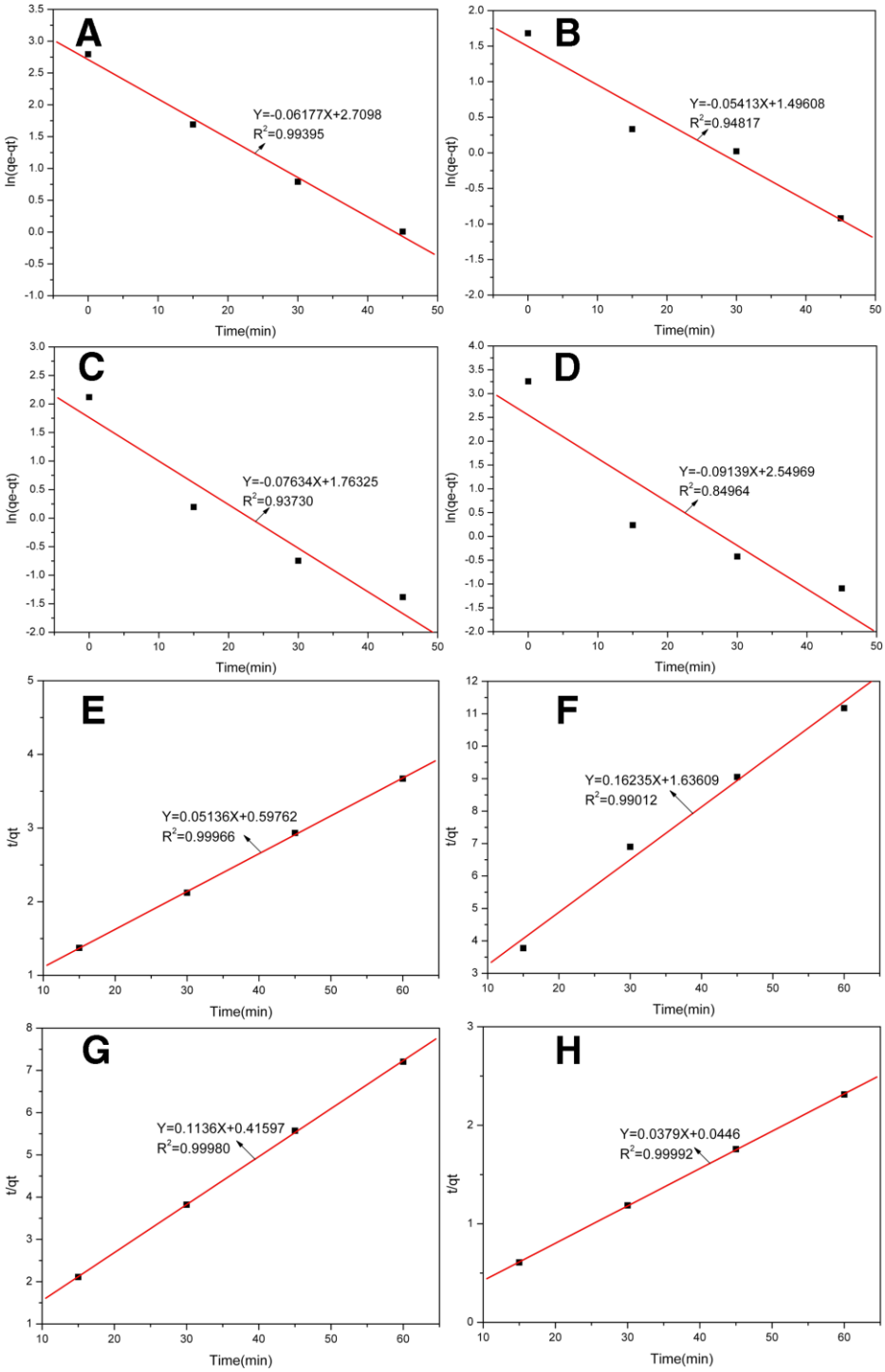

***Figure S19*.** Plots of pseudo-first-order and pseudo-second-order rates for different kinds of adsorbents and the adsorption of 50 mgL^{-1} titan yellow dye solution. The former 4 figures were fit to the pseudo-first-order model, and the latter 4 figures were fit to the pseudo-second-order model. (A) Common TiO_2; (B) Common SiO_2; (C) BH-TiO_2/SiO_2; (D) Activated carbon originating from the rice husk; (E) Common TiO_2; (F) Common SiO_2; (G) BH-TiO_2/SiO_2; (H) Activated carbon originating from the rice husk.

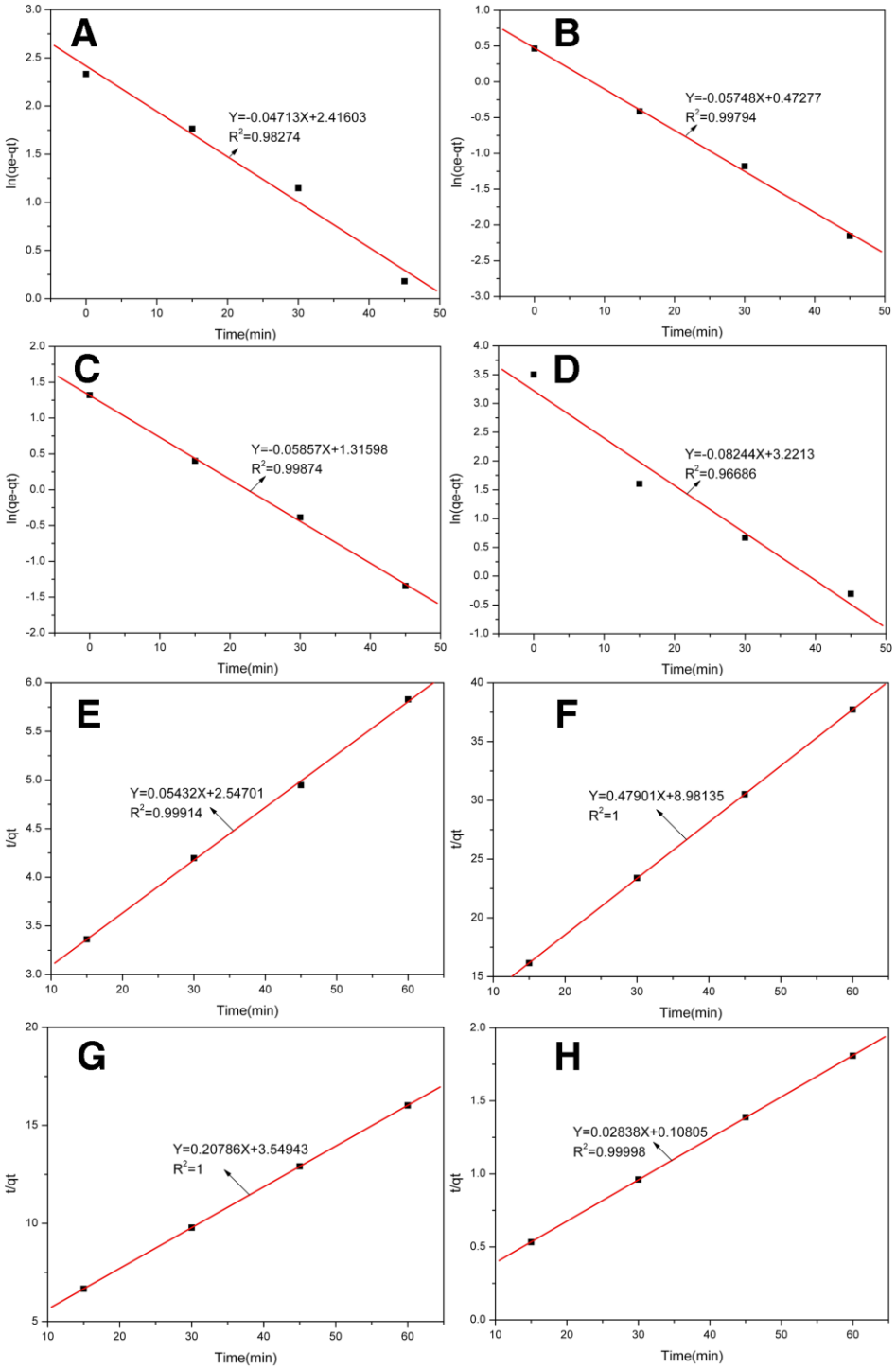

***Figure S20*.** Plots of pseudo-first-order and pseudo-second-order rates for different kinds of adsorbents and the adsorption of 75 mgL^{-1} titan yellow dye solution. The former 4 figures were fit to the pseudo-first-order model, and the latter 4 figures were fit to the pseudo-second-order model. (A) Common TiO_2; (B) Common SiO_2; (C) BH-TiO_2/SiO_2; (D) Activated carbon originating from the rice husk; (E) Common TiO_2; (F) Common SiO_2; (G) BH-TiO_2/SiO_2; (H) Activated carbon originating from the rice husk.

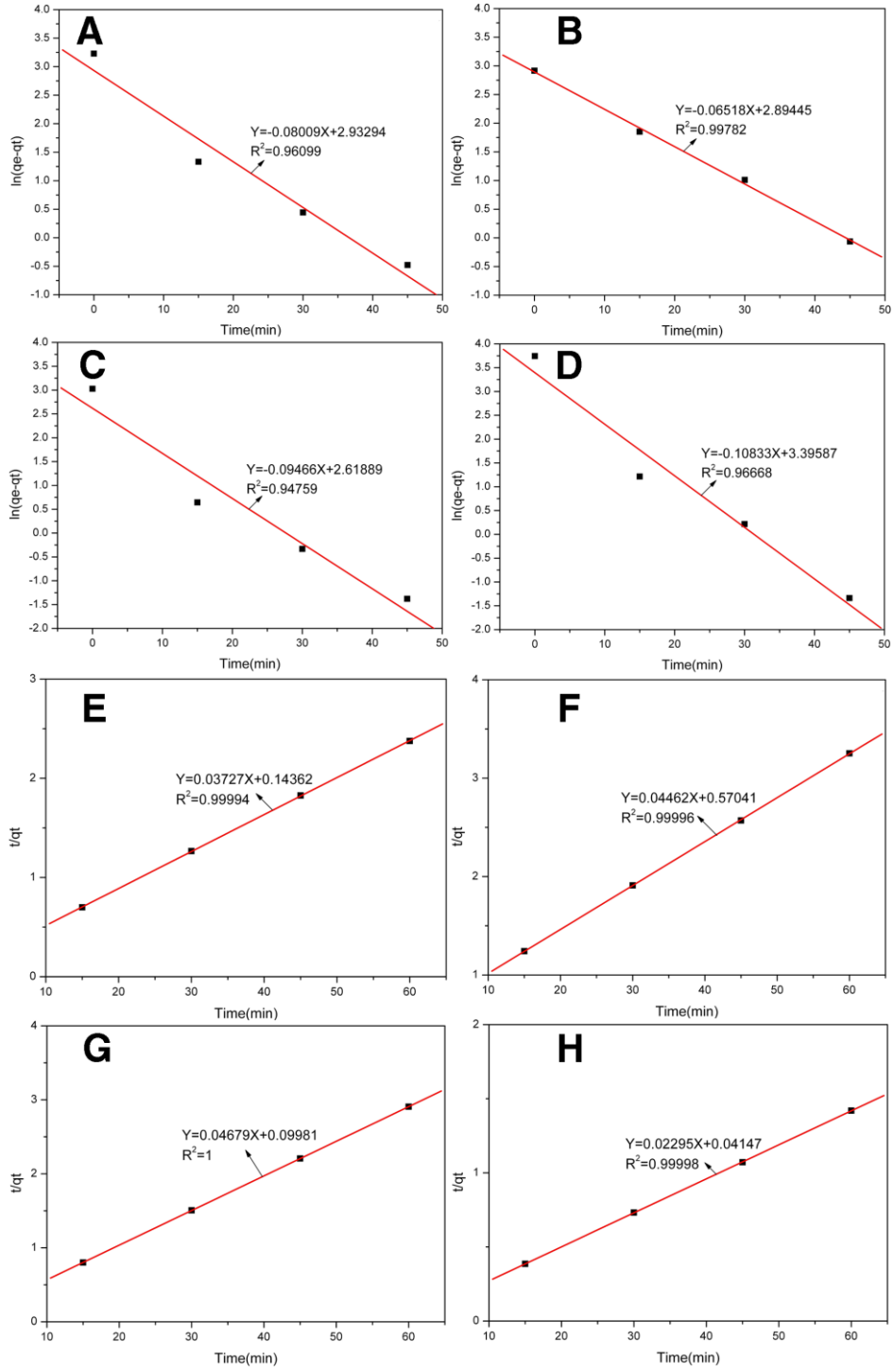

Figure S21. Plots of pseudo-first-order and pseudo-second-order rates for different kinds of adsorbents and the adsorption of 100 mgL^{-1} titan yellow dye solution. The former 4 figures were fit to the pseudo-first-order model, and the latter 4 figures were fit to the pseudo-second-order model. (A) Common TiO_2; (B) Common SiO_2; (C) BH-TiO_2/SiO_2; (D) Activated carbon originating from the rice husk; (E) Common TiO_2; (F) Common SiO_2; (G) BH-TiO_2/SiO_2; (H) Activated carbon originating from the rice husk.

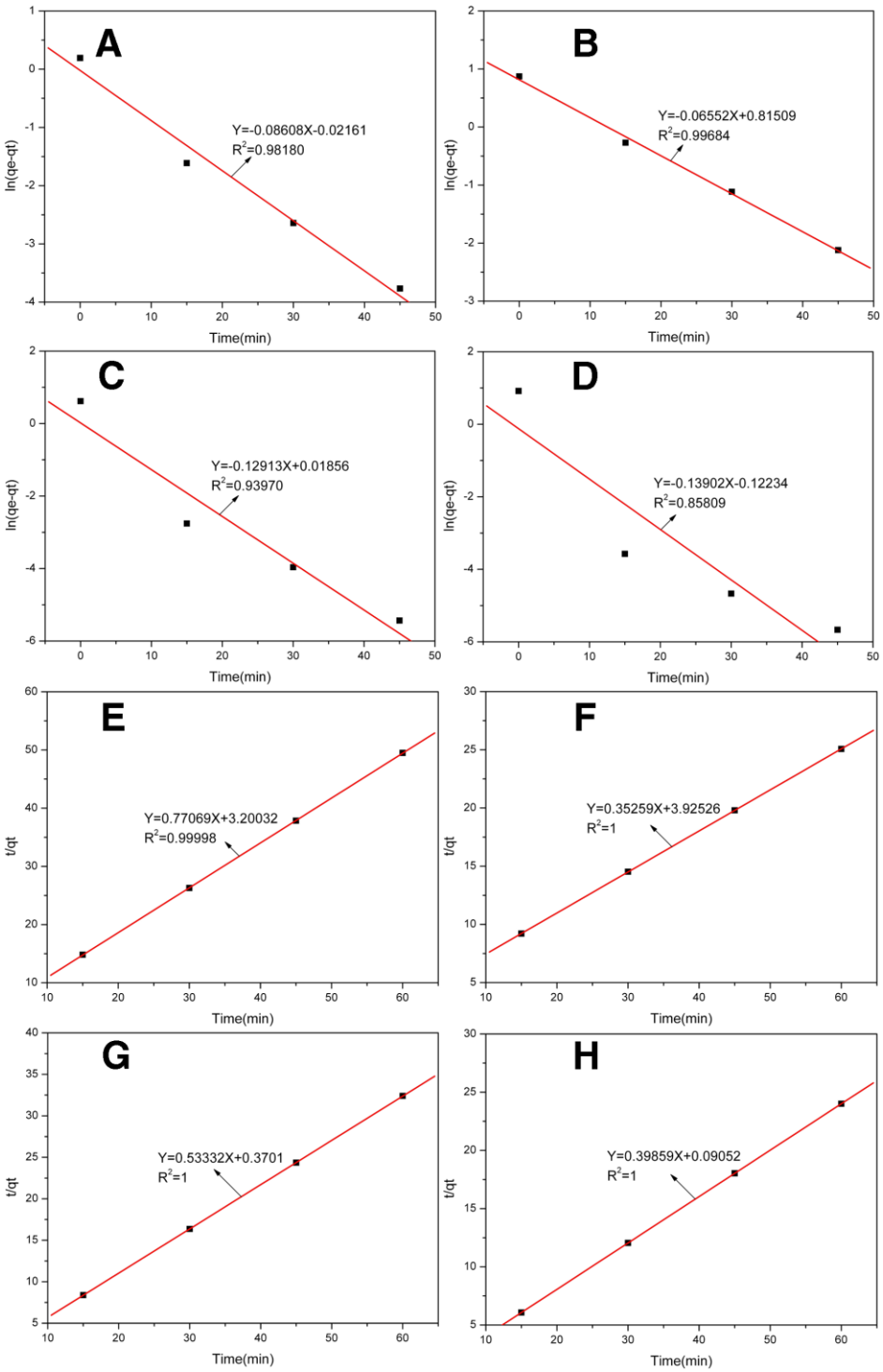

Figure S22. Plots of pseudo-first-order and pseudo-second-order rates for different kinds of adsorbents and the adsorption of 2.5 mgL^{-1} methylene blue dye solution. The former 4 figures were fit to the pseudo-first-order model, and the latter 4 figures were fit to the pseudo-second-order model. (A) Common TiO_2; (B) Common SiO_2; (C) BH-TiO_2/SiO_2; (D) Activated carbon originating from the rice husk; (E) Common TiO_2; (F) Common SiO_2; (G) BH-TiO_2/SiO_2; (H) Activated carbon originating from the rice husk.

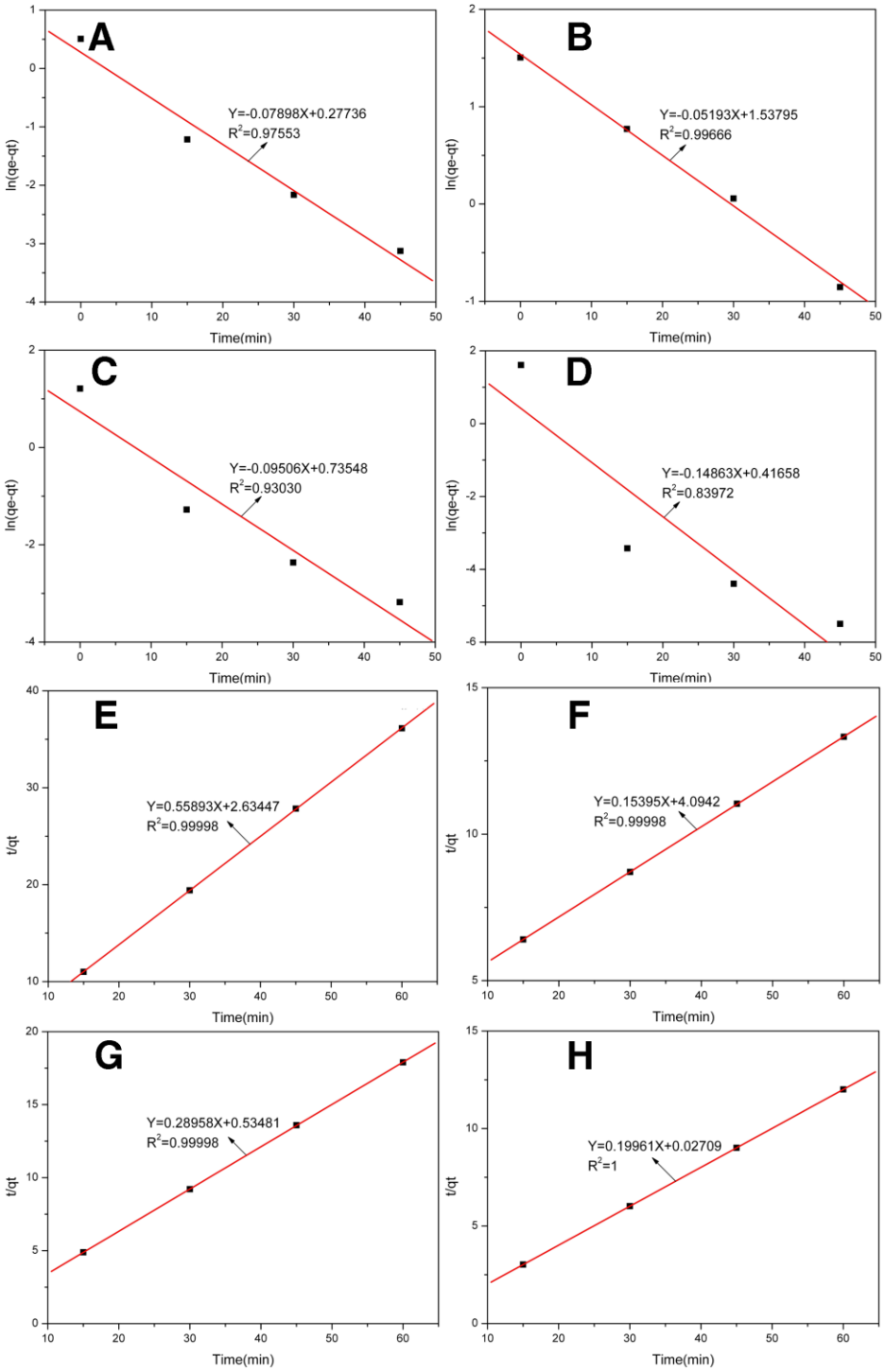

***Figure S23*.** Plots of pseudo-first-order and pseudo-second-order rates for different kinds of adsorbents and the adsorption of 5 mgL^{-1} methylene blue dye solution. The former 4 figures were fit to the pseudo-first-order model, and the latter 4 figures were fit to the pseudo-second-order model. (A) Common TiO_2; (B) Common SiO_2; (C) BH-TiO_2/SiO_2; (D) Activated carbon originating from the rice husk; (E) Common TiO_2; (F) Common SiO_2; (G) BH-TiO_2/SiO_2; (H) Activated carbon originating from the rice husk.

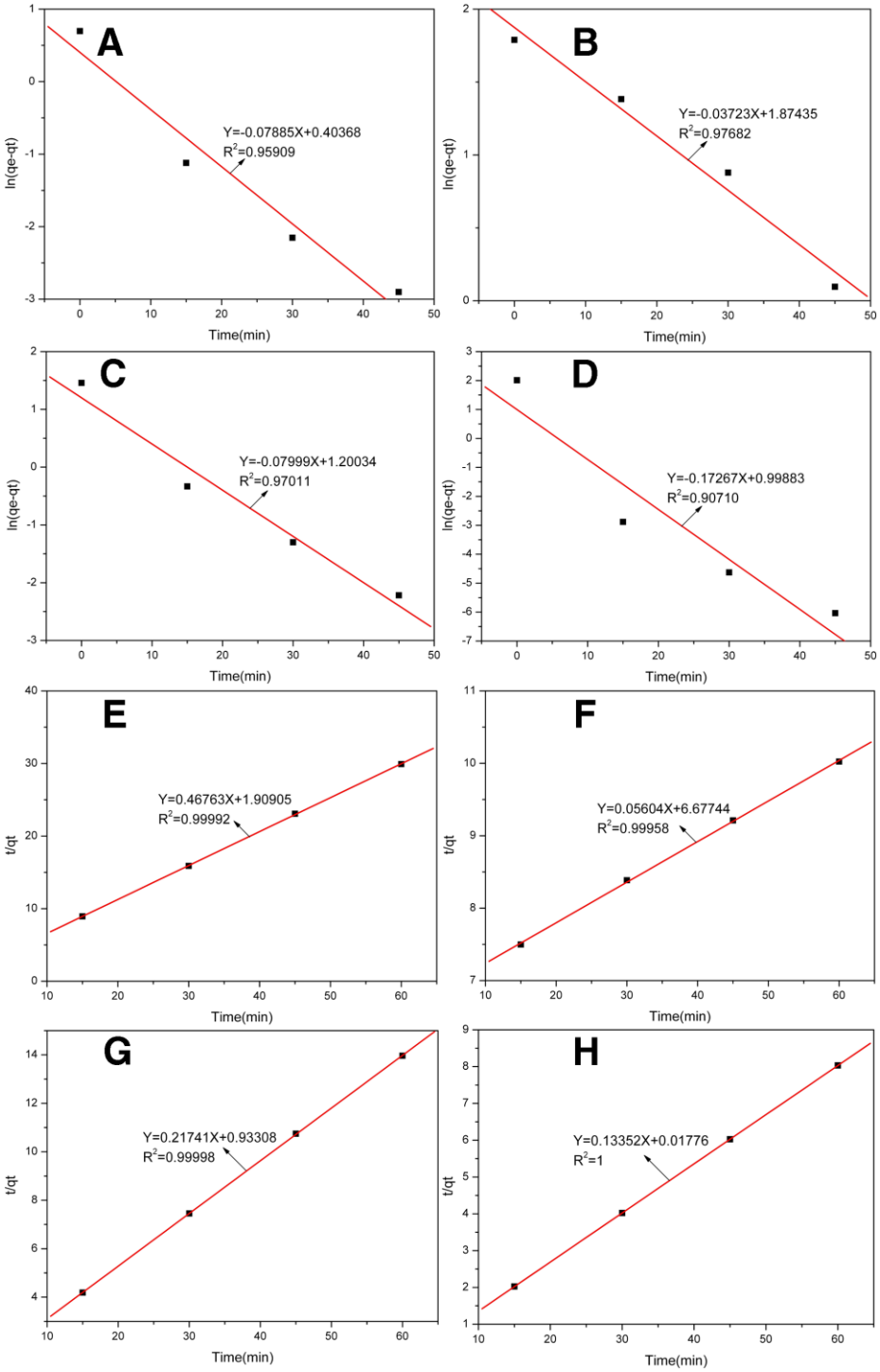

***Figure S24*.** Plots of pseudo-first-order and pseudo-second-order rates for different kinds of adsorbents and the adsorption of 7.5 mgL^{-1} methylene blue dye solution. The former 4 figures were fit to the pseudo-first-order model, and the latter 4 figures were fit to the pseudo-second-order model. (A) Common TiO_2; (B) Common SiO_2; (C) BH-TiO_2/SiO_2; (D) Activated carbon originating from the rice husk; (E) Common TiO_2; (F) Common SiO_2; (G) BH-TiO_2/SiO_2; (H) Activated carbon originating from the rice husk.

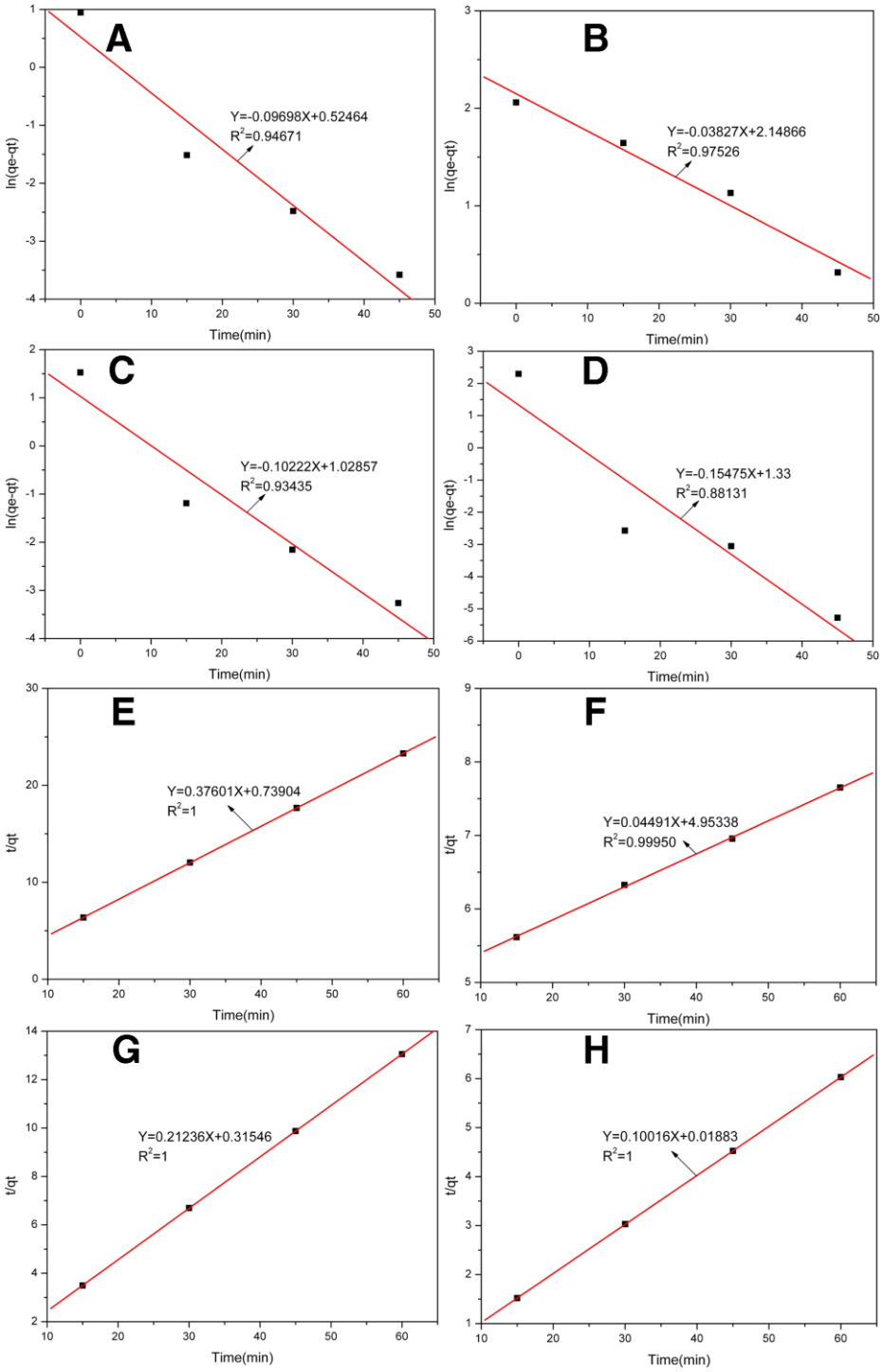

***Figure S25*.** Plots of pseudo-first-order and pseudo-second-order rates for different kinds of adsorbents and the adsorption of 10 mgL^{-1} methylene blue dye solution. The former 4 figures were fit to the pseudo-first-order model, and the latter 4 figures were fit to the pseudo-second-order model. (A) Common TiO_2; (B) Common SiO_2; (C) BH-TiO_2/SiO_2; (D) Activated carbon originating from the rice husk; (E) Common TiO_2; (F) Common SiO_2; (G) BH-TiO_2/SiO_2; (H) Activated carbon originating from the rice husk.

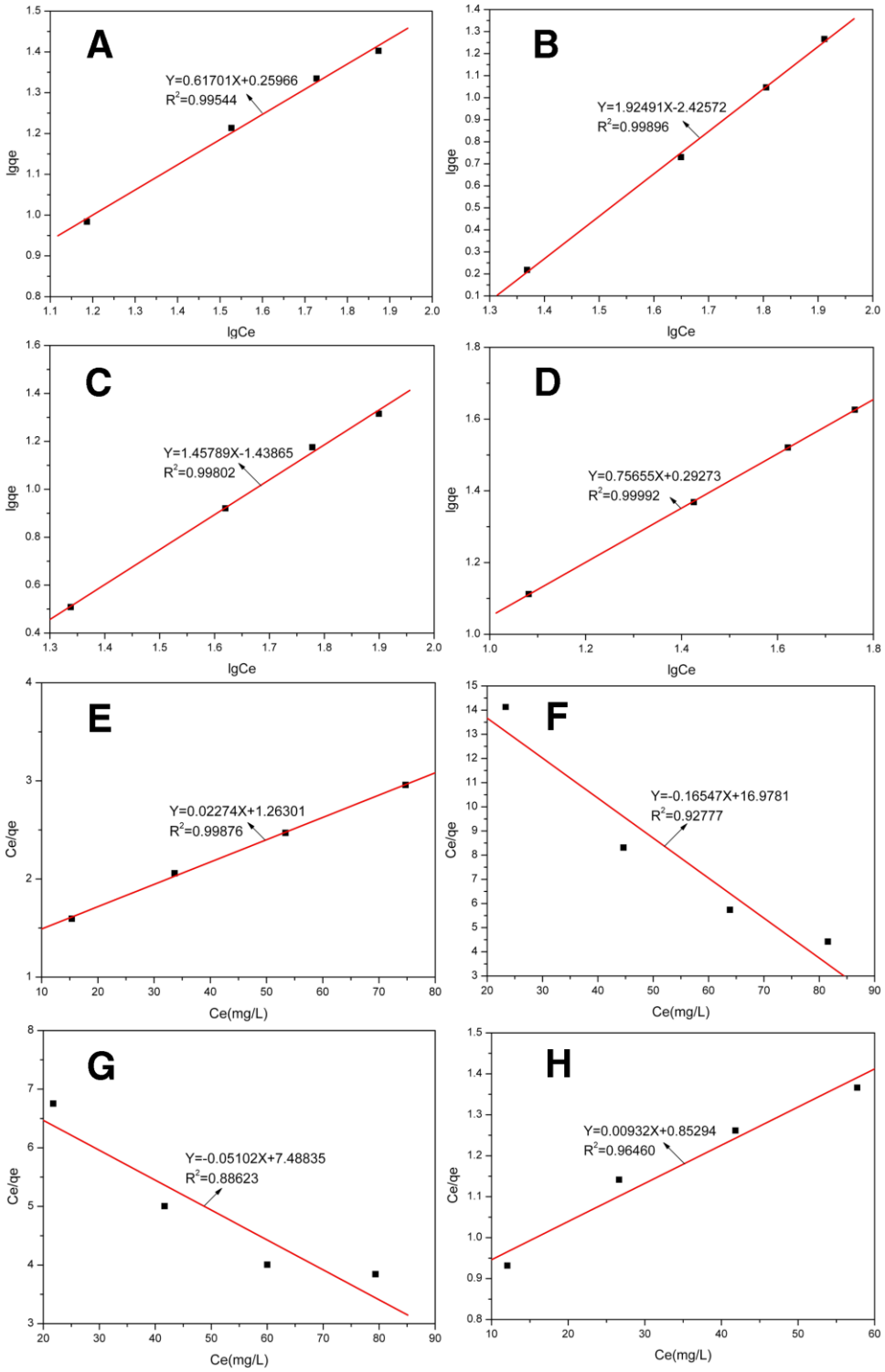

Figure S26. Adsorption isotherms for titan yellow. The former 4 figures were fit to the Freundlich model and the latter 4 figures were fit to the Langmuir model. (A) Common TiO_2; (B) Common SiO_2; (C) BH-TiO_2/SiO_2; (D) Activated carbon originating from the rice husk; (E) Common TiO_2; (F) Common SiO_2; (G) BH-TiO_2/SiO_2; (H) Activated carbon originating from the rice husk.

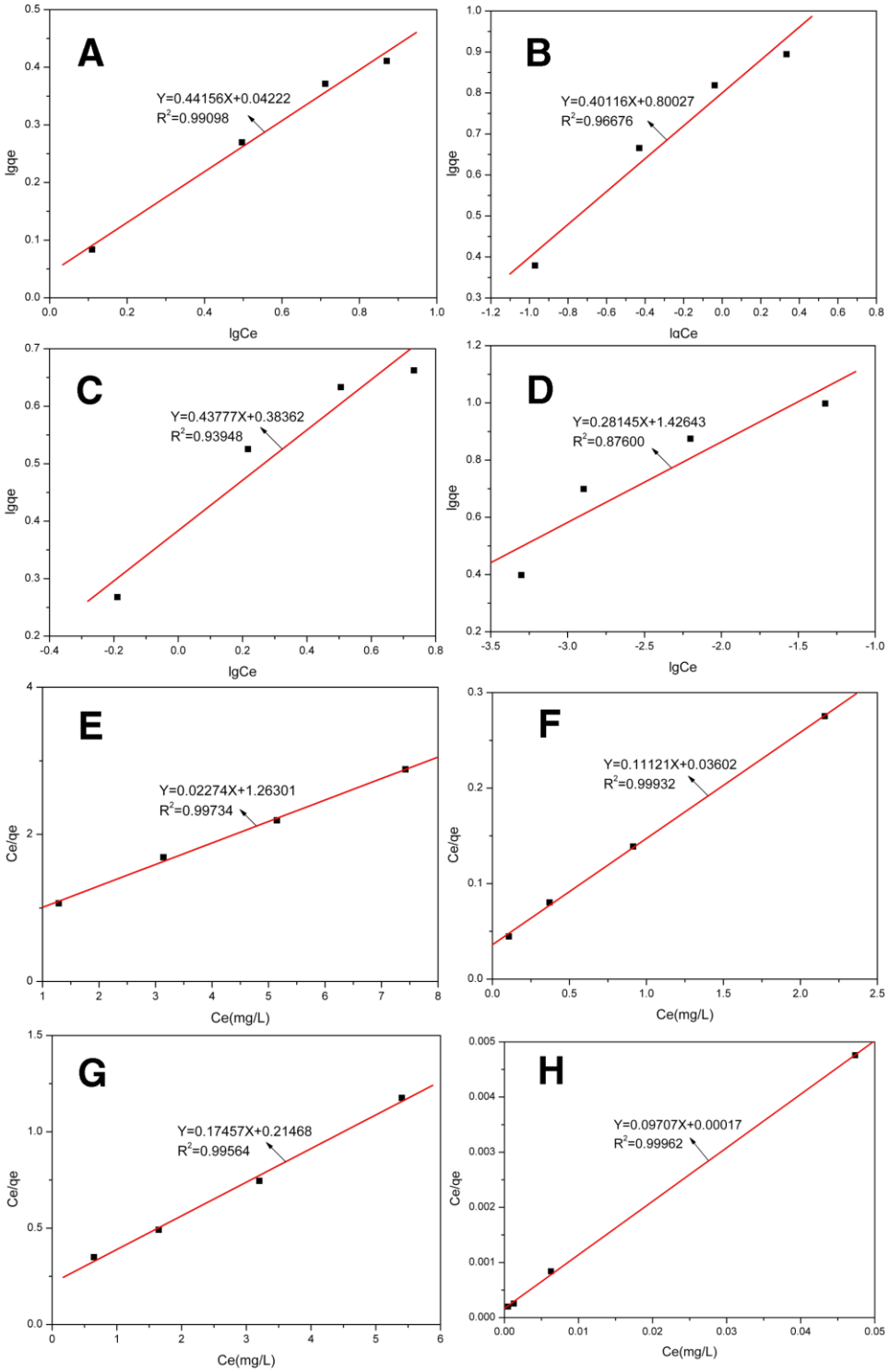

Figure S27. Adsorption isotherms for methylene blue. The former 4 figures were fit to the Freundlich model and the latter 4 figures were fit to the Langmuir model. (A) Common TiO_2; (B) Common SiO_2; (C) BH-TiO_2/SiO_2; (D) Activated carbon originating from the rice husk; (E) Common TiO_2; (F) Common SiO_2; (G) BH-TiO_2/SiO_2; (H) Activated carbon originating from the rice husk.

Table S1. Number of the *E. coli* colonies in 1 μL solution diluted 10^4 times.

Sample\Type	1	2	3	Average[f]	Efficiency(%)[g]
0[a]	141	114	88	114.3±26.5	0
1[b]	60	55	48	54.3±6.0	52.5
2[c]	120	75	101	98.7±22.6	13.7
3[d]	25	15	18	19.3±5.1	83.1
4[e]	46	48	40	44.7±4.2	60.9

[a] The filtrate obtained without absorbents, in triplicate. [b] The filtrate obtained under the adsorption effect of common TiO_2, in triplicate. [c] The filtrate obtained under the adsorption effect of common SiO_2, in triplicate. [d] The filtrate obtained under the adsorption effect of BH-TiO_2/SiO_2, in triplicate. [e] The filtrate obtained under the adsorption effect of activated carbon originating from the rice husk, in triplicate. [f] The average count's error is the standard deviation of 3 results. [g] The efficiency is the *E. coli* physical removal efficiencies for absorbents.

Table S2. Number of the *E. coli* colonies in 0.1 mL solution diluted to 10^4 times.

Sample\Type	1	2	3	Average[f]	Efficiency(%)[g]
0[a]	372	389	338	366.3±26.0	0
1[b]	354	282	392	342.7±55.9	6.5
2[c]	287	224	313	274.7±45.8	25.0
3[d]	33	46	33	37.3±7.5	89.8
4[e]	205	166	138	169.7±33.7	53.7

[a] The solution that was not under the bacteriostatic effect of the samples, in triplicate. [b] The solution that was under the bacteriostatic effect of common TiO_2, in triplicate. [c] The solution that was under the bacteriostatic effect of common SiO_2, in triplicate. [d] The solution that was under the bacteriostatic effect of BH-TiO_2/SiO_2, in triplicate. [e] The solution that was under the bacteriostatic effect of activated carbon originating from the rice husk, in triplicate. [f] The average count's error is the standard deviation of 3 results. [g] The efficiency is the *E. coli* bacteriostatic efficiencies for different samples.

Table S3. Number of the *E. coli* colonies in 0.1 mL solution without samples diluted 10^4 times and 0.1 mL solution with different samples diluted 10^3 times.

Sample\Type	1	2	3	Average[g]	Efficiency(%)[h]
0[a]	438	561	710	569.7±136.2	0
0^+[b]	184	88	75	115.7±59.5	79.7
1[c]	58	61	42	53.7±10.2	99.1
2[d]	106	75	47	76.0±29.5	98.7
3[e]	33	46	33	37.3±7.5	99.3
4[f]	200	172	122	164.7±39.5	97.1

[a] The solution without samples that was not under UV irradiation, in triplicate. [b] The solution without samples that was under UV irradiation, in triplicate. [c] The solution with common TiO_2 that was under UV irradiation, in triplicate. [d] The solution with common SiO_2 that was under UV irradiation, in triplicate. [e] The solution with BH-TiO_2/SiO_2 that was under UV irradiation, in triplicate. [f] The solution with activated carbon originating from the rice husk that was under UV irradiation, in triplicate. [g] The average count's error is the standard deviation of 3 results. [h] The efficiency is the *E. coli* chemical removal efficiencies by different samples' properties under UV irradiation.

Table S4. Number of the *E. coli* colonies in 0.1 mL solution diluted 10^4 times.

Sample\Type	1	2	3	Average[g]	Efficiency(%)[h]
0[a]	122	122	134	126±6.9	0
0^+[b]	898	1300	1059	1085.7±202.3	761.7
1[c]	989	1424	1075	1162.7±230.4	822.8
2[d]	1201	998	1438	1212.3±220.2	862.1
3[e]	775	852	797	808.0±39.7	541.3
4[f]	1812	2102	1771	1895.0±180.4	1404.0

[a] The solution without samples that was not under visible light irradiation, in triplicate. [b] The solution without samples that was under visible light irradiation, in triplicate. [c] The solution with common TiO_2 that was under visible light irradiation, in triplicate. [d] The solution with common SiO_2 that was under visible light irradiation, in triplicate. [e] The solution with BH-TiO_2/SiO_2 that was under visible light irradiation, in triplicate. [f] The solution with activated carbon originating from the rice husk that was under visible light irradiation, in triplicate. [g] The average count's error is the standard deviation of 3 results. [h] The efficiency is the *E. coli* growth efficiencies by different samples' properties under visible light irradiation.